AD-A011 438

THE MEAN AND OSCILLATORY FORCES ON A HYDROFOIL WITH COMBINED NATURAL AND FORCED VENTILATION FROM EXPERIMENTS IN REGULAR WAVES

R. Stahl, et al

Naval Ship Research and Development Center
Bethesda, Maryland

May 1975

DISTRIBUTED BY:

NTIS

National Technical Information Service
U. S. DEPARTMENT OF COMMERCE

189149

SPD 626-01

ADA011438

NAVAL SHIP RESEARCH AND DEVELOPMENT CENTER

Bethesda, Maryland 20084

THE MEAN AND OSCILLATORY FORCES ON A HYDROFOIL WITH COMBINED NATURAL AND FORCED VENTILATION FROM EXPERIMENTS IN REGULAR WAVES

by

R. STAHL

and

E. E. ZARNICK

APPROVED FOR PUBLIC RELEASE: DISTRIBUTION UNLIMITED

SHIP PERFORMANCE DEPARTMENT

Reproduced by
NATIONAL TECHNICAL
INFORMATION SERVICE
US Department of Commerce
Springfield, VA. 22151

MAY 1975

SPD 626-01

THE MEAN AND OSCILLATORY FORCES ON A HYDROFOIL WITH COMBINED
NATURAL AND FORCED VENTILATION FROM EXPERIMENTS IN REGULAR WAVES

UNCLASSIFIED

SECURITY CLASSIFICATION OF THIS PAGE (When Data Entered)

REPORT DOCUMENTATION PAGE		READ INSTRUCTIONS BEFORE COMPLETING FORM
1 REPORT NUMBER SPD 626-01	2. GOVT ACCESSION NO.	3 RECIPIENT'S CATALOG NUMBER
4 TITLE (and Subtitle) THE MEAN AND OSCILLATORY FORCES ON A HYDROFOIL WITH COMBINED NATURAL AND FORCED VENTILATION FROM EXPERIMENTS IN REGULAR WAVES		5 TYPE OF REPORT & PERIOD COVERED FINAL 6. PERFORMING ORG. REPORT NUMBER
7 AUTHOR(s) R. STAHL E. E. ZARNICK		8 CONTRACT OR GRANT NUMBER(s)
9 PERFORMING ORGANIZATION NAME AND ADDRESS SHIP PERFORMANCE DEPARTMENT NAVAL SHIP RESEARCH AND DEVELOPMENT CENTER BETHESDA, MARYLAND 20084		10 PROGRAM ELEMENT, PROJECT, TASK AREA & WORK UNIT NUMBERS Work Unit 1520-001 Program No. 62754N Task Area ZF43421001, W.U.
11 CONTROLLING OFFICE NAME AND ADDRESS NAVAL MATERIAL COMMAND WASHINGTON, D. C. 20360		12. REPORT DATE MAY 1975 13. NUMBER OF PAGES 52
14 MONITORING AGENCY NAME & ADDRESS(if different from Controlling Office)		15. SECURITY CLASS. (of this report) UNCLASSIFIED 15a. DECLASSIFICATION/DOWNGRADING SCHEDULE

16 DISTRIBUTION STATEMENT (of this Report)

APPROVED FOR PUBLIC RELEASE: DISTRIBUTION UNLIMITED

17 DISTRIBUTION STATEMENT (of the abstract entered in Block 20, if different from Report)

18. SUPPLEMENTARY NOTES

PRICES SUBJECT TO CHANGE

19. KEY WORDS (Continue on reverse side if necessary and identify by block number)

Ventilated Hydrofoil in Waves
Natural Ventilated Foil, Forced
Ventilated Foil, Mean Lift
Mean Drag, Oscillatory Lift
Oscillatory Drag

20. ABSTRACT (Continue on reverse side if necessary and identify by block number)

An experimental investigation was made to determine the mean and oscillatory lift and drag forces on a hydrofoil with combined natural and forced ventilation in regular waves. Natural ventilation was provided by the addition of wedges to the after end of the foil strut. Forced ventilation was provided by blowing air through slots in the upper surface of the foil. The experiments were conducted with the foil operating in regular waves of several different lengths at various speeds and foil depths. Most of the experiments

DD FORM 1 JAN 73 1473 EDITION OF 1 NOV 65 IS OBSOLETE
S/N 0102-014-6601

UNCLASSIFIED

SECURITY CLASSIFICATION OF THIS PAGE (When Data Entered)

The Naval Ship Research and Development Center is a U. S. Navy center for laboratory effort directed at achieving improved sea and air vehicles. It was formed in March 1967 by merging the David Taylor Model Basin at Carderock, Maryland with the Marine Engineering Laboratory at Annapolis, Maryland.

Naval Ship Research and Development Center

Bethesda, Md. 20034

MAJOR NSRDC ORGANIZATIONAL COMPONENTS

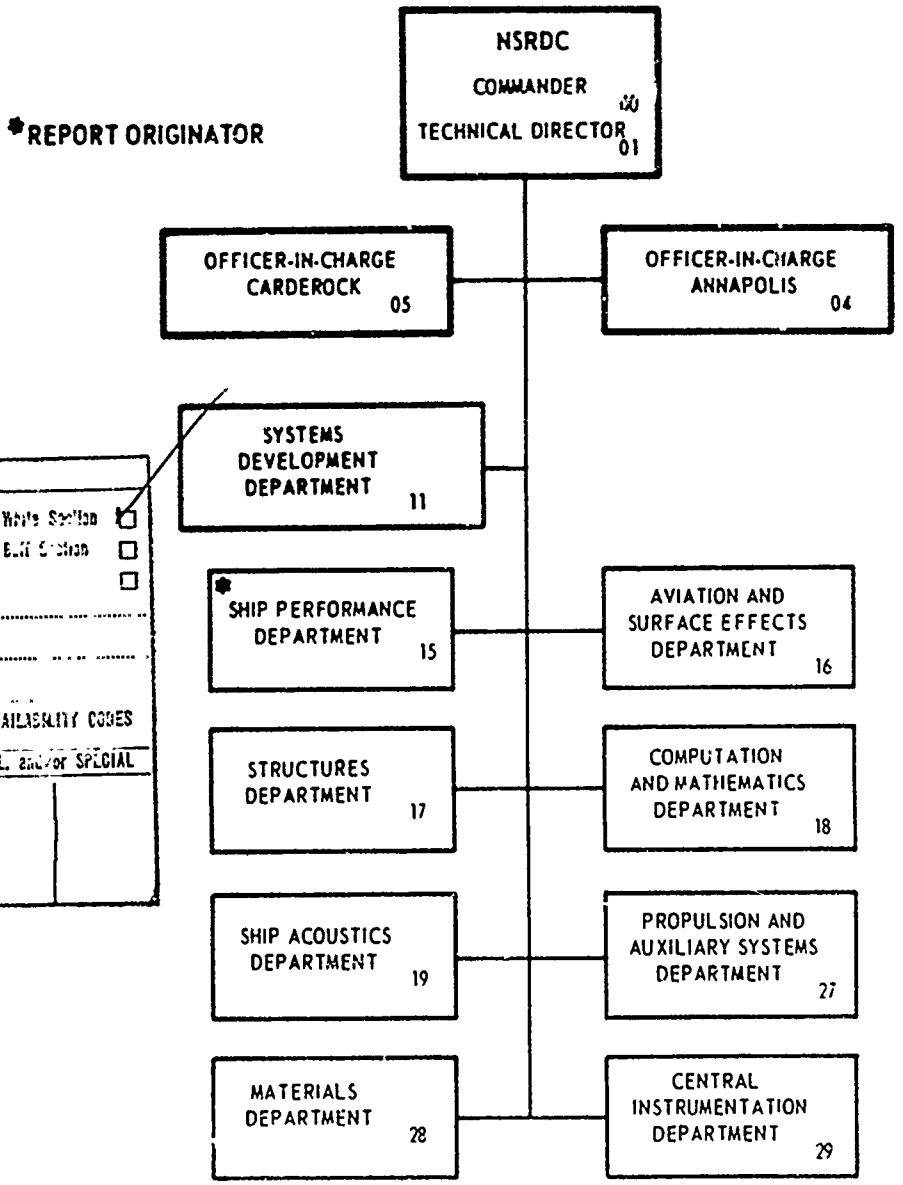

ACCESSION for
NTIS White Section
D D Buff Section
UNANNOUNCED
JUSTIFICATION
BY
DISTRIBUTION/AVAILABILITY CODES
Dist. AVAIL. and/or SPECIAL

NDW-NSRDC 3960/46 (REV. 8-71)
GPO 888-234

(continued)

were conducted in head waves but some data were obtained in following waves. Results are presented showing the variation of the mean and oscillatory components of cavitation number based on cavity pressure, lift coefficient and drag coefficient with ventilation index (a measurement of the air flow rate).

NOTATION

A_p	Projected area of the foil perpendicular to the direction of the carriage velocity, i.e., on a horizontal plane
A_t	Area of hydrofoil trailing edge surface
$\overline{C}_L$	Mean lift coefficient
$\Delta C_L/\Delta\alpha$	Oscillatory lift coefficient in waves
$C_{L,d}$	Section design lift coefficient for $\alpha = 0$
$\overline{C}_D$	Mean drag coefficient
$\Delta C_D/\Delta\alpha$	Oscillatory drag coefficient in waves
c	Mean chord length of the hydrofoil
$\overline{D}_m$	Mean measured drag
ΔD_m	Amplitude of measured oscillatory drag
d	Foil depth, measured between the mean free waterplane and the leading edge of the mid section
ζ	Wave amplitude
K_v	Ventilation index Q/VA_p
k	Wave number $2\pi/\lambda$
$\overline{L}$	Mean measured lift
ΔL	Amplitude of measured oscillatory lift
p_∞	Free-stream static pressure
p_c	Measured cavity pressure
p_a	Atmospheric pressure
p_m	Measured pressure at flowmeter
Q	Force ventilating volumetric flow of equivalent mass of air at atmospheric pressure
Q_m	Measured volume rate of air-flow

NOTATION (continued)

q	Free-stream dynamic pressure, $\rho V^2/2$
S	Plan form area of the hydrofoil, 0.333 ft.^{2}
s	Hydrofoil span
V	Speed
x,y	Coordinate axes with origin at strut leading edge
α	Foil angle of attack, measured between the reference plane of the hydrofoil and horizontal plane
α_{NT}	Foil angle of attack, measured between the nose-tail line of the foil and a horizontal plane
$\Delta\alpha$	Change in angle of attack due to the orbital velocity of water particles in waves, $(\zeta\omega_o e^{-kd})/V$
λ	Wavelength
ρ	Density of water
σ_c	Cavitation number, $(p_\infty - p_c)/q$
τ	Foil Taper ratio, $c_{tip}/c_{midspan}$
ω_o	Circular frequency of wave

TABLE OF CONTENTS

	Page
ABSTRACT	1
ADMINISTRATIVE INFORMATION	1
INTRODUCTION	2
DESCRIPTION OF MODEL	3
EXPERIMENTAL APPARATUS	4
EXPERIMENTAL PROCEDURE	6
PRESENTATION AND DISCUSSION OF EXPERIMENTAL RESULTS	8
GENERAL	8
MEAN CAVITATION NUMBER	10
MEAN LIFT AND DRAG	14
OSCILLATORY LIFT AND DRAG	16
SUMMARY AND CONCLUSIONS	18
ACKNOWLEDGMENTS	19
REFERENCES	20
APPENDIX - DATA REDUCTION	21

LIST OF FIGURES

	Page
Figure 1 - Hydrofoil H47	24
Figure 2 - Hydrofoil-Strut Orientation with Coordinate Axis	25
Figure 3 - Hydrofoil Strut Offsets and Geometry	26
Figure 4 - Variation of Cavitation Number with Ventilation Index in Calm Water	27
Figure 5 - Variation of Mean Cavitation Number with Ventilation Index in Regular Waves	28
Figure 6 - Variation of Lift Coefficient with Ventilation Index in Calm Water	30
Figure 7 - Variation of Mean Lift Coefficient with Ventilation Index in Regular Waves	31
Figure 8 - Variation of Lift Coefficient with Cavitation Number in Calm Water	32
Figure 9 - Variation of Mean Lift Coefficient with Mean Cavitation Number in Regular Waves	33
Figure 10 - Variation of Drag Coefficient with Cavitation Number in Calm Water	37
Figure 11 - Variation of Mean Drag Coefficient with Mean Cavitation Number in Regular Waves	38
Figure 12 - Variation of Oscillatory Lift Coefficient with Ventilation Index in Regular Waves	41
Figure 13 - Variation of Oscillatory Drag Coefficient with Ventilation Index in Regular Waves	43

ABSTRACT

An experimental investigation was made to determine the mean and oscillatory lift and drag forces on a hydrofoil with combined natural and forced ventilation in regular waves. Conditions for natural ventilation were enhanced by the addition of wedges to the after end of the foil strut. Forced ventilation was provided by blowing air through slots in the upper surface of the foil. The experiments were conducted with the foil operating in regular waves of several different lengths at various speeds and foil depths. Most of the experiments were conducted in head waves, but some data were obtained in following waves. Results are presented showing the variation of the mean and oscillatory components of cavitation number based on cavity pressure, lift coefficient and drag coefficient with ventilation index (a measurement of the air flow rate).

ADMINISTRATIVE INFORMATION

This work was supported by the Naval Material Command under Program Element 62754N, Task Area ZF 43421001, known as the High Speed Struts and Foils Direct Laboratory Funded Project.

INTRODUCTION

In some regions of operation of a hydrofoil, it may be desirable to control the cavitation number in order to control the lift or to balance and improve lift-drag characteristics over a broad speed range from wetted flow to supercavitating conditions. A means of controlling the cavitation number is the introduction of a gas (usually air) to the upper surface or wake of the foil, thus forming a fully developed cavity which would not normally exist. The air can be supplied naturally through a direct path to the atmosphere as provided, for example, by a base vented strut, or it can be provided artificially by forcing gas through slots in the upper surface of the foil.

As part of a hydrofoil Task Area Plan, an exploratory investigation was made of a strut-foil system incorporating both natural and forced ventilation of cavity. Specifically, experiments were conducted to investigate the performance of a foil with combined forced and natural ventilation in regular waves and to determine the corresponding oscillatory lift and drag components. Natural ventilation was aided by the addition of wedges to the after end of the foil strut. Forced ventilation was provided by blowing air through slots in the upper surface of the foil.

The experiments were conducted with the foil operating in waves of several different lengths and at various speeds and foil depths. Most of the experiments were conducted in head waves, but some data were obtained in following waves. Also, some data were obtained without wedges on the strut. The results are presented in this report showing the variation of

the mean and oscillatory components of the cavitation number, lift coefficient and drag coefficients with the ventilation index.

DESCRIPTION OF MODEL

The model chosen for the investigation of forced ventilation was an existing tapered hydrofoil, NSRDC Foil No. H47, see Reference 1 and Figure 1.[1] The plan area of the model foil was 48 square inches with a 5.33-inch maximum chord length at midspan and a taper ratio τ of 0.50, where $\tau = \frac{c_{tip}}{c_{root}} = \frac{\text{chord length at tip}}{\text{chord length at midspan}}$. Upper and lower surfaces were generated from geometrically similar two-dimensional sections having a common reference plane resulting in a spanwise taper with a maximum foil thickness at midspan. The sections geometrically had a Tulin-Burkhart two-term camber corresponding to a section lift coefficient $C_{L,d}$ of 0.2. Coinciding with the upper surface of the sections was the theoretical cavity shape at an attack angle α_{NT} of 3.69 degrees at a cavitation number σ_c of 0, and a submergence depth d of ∞ (Reference 1). Subsequent reference to hydrofoil angle of attack, α, will be the angle between the foils reference plane and a horizontal plane, Figure 2.

The hydrofoil was supported by a single strut whose geometry and offsets are shown in Figure 3. Gemoetrically, the strut sections were similar to NACA 16-012 airfoil sections except for a non-streamlined wedge-like modification located between $0.500 \leq x/c \leq 0.700$ at the base

[1] References are listed on page 20

of the strut and continuing upward parallel to the leading edge for an overall length of 22 inches on both sides of the strut. The wedge section was 0.80 inches long with a trailing edge thickness of 0.135 inches. The material of the streamlined portion of the strut was stainless steel whereas the wedges were epoxy. Geometrically, the upper strut portion of the hydrofoil was a continuation of the lower 10-inch long cylindrical strut with expanded chord and thickness.

Fourteen ventilation holes were located on the top surface of the foil symmetrically about the midspan, Figure 1. An air duct inside the foil linked the fourteen ventilation ports with a duct running inside the strut. Near the top of the strut the duct was connected via pipes and hoses to a flowmeter and a suitable air supply.

In order to accommodate the electrical leads for a pressure transducer mounted on the foil's trailing edge, (i.e. on the base of the wedge-shaped foil) a groove was machined into one side of the strut and a hole was drilled into the foil leading from the strut to the transducer. The groove with the transducer leads inside was covered partly by a strip of stainless steel and partly by an epoxy fill-in, both of which were sanded for a restoration of the intended geometry of strut and hydrofoil.

EXPERIMENTAL APPARATUS

The facility used was the Center's 21-foot wide, 2968-foot long high-speed towing basin having a minimum water depth of 7.5 feet. Water in the basin was fresh with a temperature deviating only slightly from 70°F. A pneumatic wavemaker at one end of the basin permitted the generation

of regular waves which ranged in these experiments from 16-inch high, 40-foot long waves to 6-inch high, 15-foot long waves. The model was towed by Carriage 5 at a maximum straight-line speed of 34.9 ft/sec.

Mounting the hydrofoil required a means of adjusting the model for the desired depth of submergence and angle of attack with a resonable degree of rigidity. For this, an existing yaw table was utilized in conjunction with the carriage-mounted vertical rails and electromechanical hoisting system. A lift-drag dynamometer consisting of two separate assemblies of two modular force gages (lift and drag) using differential reluctance transducers was mounted to the underside of the yaw table with appropriate attachments to provide the degrees of freedom necessary to remove couplings and avoid erroneous force measurements. The two 4-inch lift-measuring block gages and the two 4-inch drag-measuring block gages were oriented in line with the direction of carriage travel. Mounted below the dynamometer was an adjustable pitch plate (to which the strut was attached), whereby the desired foil angle of attack could be obtained.

Other measured test parameters were foil depth, cavity pressure behind the foil's trailing edge, wave amplitude, carriage speed, and the rate at which air was supplied to the foil's upper surface. The corresponding transducers used were a linear potentiometer for foil depth, a small strain gaged pressure transducer mounted on the back side of the trailing foil surface and within the anticipated cavity, an ultrasonic wave probe mounted forward of the model where approaching

waves were unaffected by the model, a reluctance pulse pickup for carriage speed, and a flowmeter-pressure-temperature gage system for determining the volumetric air flow. Bottled compressed air was supplied to, and metered by, a Fischer-Porter "Flowrator" with a maximum input pressure of 200 psig. A pressure gage located at the flowmeter allowed correction of the airflow readings to standard conditions. The correction used, which was based on the Flowrator characteristics, was

$$Q = Q_m \frac{p_a + p_m}{p_a}$$

where Q_m = measured volume rate of flow, ft^3/min.

Q = volumetric flow of equivalent mass of air at atmospheric pressure, ft^3/min.

p_a = atmospheric pressure, psia

p_m = measured gage pressure, psig

The amplified transducer signals (including the sums of the two lift measuring gages and of the two drag measuring gages) were recorded on strip chart and analog magnetic tape. The signals were also analyzed on the carriage during the test, utilizing the Interdata computer system, and recorded on digital magnetic tape for post-test analysis.

EXPERIMENTAL PROCEDURE

The program for investigating unsteady effects on high speed hydrofoils in regular waves with combined forced and natural ventilation consisted of experiments in calm water, regular head waves, and regular following waves.

The program was conducted with various combinations of hydrofoil depth of submergence/mean chord ratio (d/c), angle of attack (α), speed (V), and air flow rate (Q) to the foil's upper surface. In the regular wave experiments wave length and wave amplitude were also varied. These parameters varied within the following ranges model scale:

$$1.0 \leq d/c \leq 3.0$$

$$5 \leq \alpha \leq 19 \text{ (deg)}$$

$$17.4 \quad V \quad 34.9 \text{ (ft/sec)}$$

$$0 \quad Q \quad 45 \text{ (cubic ft/min)}$$

$$15 \quad \lambda \quad 40 \text{ (ft)}$$

$$3 \quad \zeta \quad 8 \text{ (in)}$$

The most frequently used wave condition was $\zeta = 3$ inches with $\lambda = 30$ or 40 feet, the corresponding wave steepnesses being 1/60 and 1/80. The speed range was selected on the basis of Froude scaling assuming a 1/15 scale ratio between model and prototype and full scale speeds from 40 to 80 knots. Since scaling associated with ventilated flow is actually more complicated than simple Froude scaling, no further reference will be made to full scale values of speed.

Each run was conducted under steady state conditions; i.e., no change was made in the foil depth below the mean water surface, foil angle of attack, carriage speed, and air flow to the foil's upper surface. Foil angle of attack and foil depth were adjusted to the desired setting prior to each passage of the carriage along the length of the basin. After the attainment of the desired steady state carriage

speed, the air flow was increased in steps with each step taken as a run. Among the objectives of the calm water phase of the program was a comparison with previous results of the same model foil but with the unmodified streamlined supporting strut (Reference 1). Foil depth in all regular wave experiments was chosen to assure continuous foil immersion. Using the various combinations of hydrofoil speed and wavelength, encounter frequencies ranged between 2.91 and 0.79 hertz in regular head waves and 0.57 to 0.08 hertz in regular following waves. Hydrofoil speed was always greater than wave celerity in the following wave runs. The final phase of the program involved the removal of the epoxy wedges on the strut whereby the original streamlined strut was restored. Experiments with this configuration were conducted in regular head waves at a single foil depth of two chords.

PRESENTATION AND DISCUSSION OF EXPERIMENTAL RESULTS

GENERAL

The behavior of the strut-foil systems was complicated by the interaction of the several different mechanisms by which the upper surface of the foil was ventilated. Ventilation could occur naturally by means of the wedges or could be forced by blowing air through openings on the upper surface of the foil. These two mechanisms of ventilation not only interacted with one another, but were also capable of triggering hyperventilation. Hyperventilation here is defined as a natural ventilation associated with the breaking open of the cavity to the atmosphere whereby air entered directly through

the downstream part of the cavity.

At the speeds examined during these experiments and without strut wedges or the occurrence of broaching, the foil appeared to operate in a fully wetted regime. The addition of wedges, however, had the predictable effect of providing a path to the atmosphere for ventilation of the foil. This was most clearly observed with the foil at an angle of attack of 10 degrees, depth of two chord lengths, and speed of 10.3 knots. A fully developed cavity existed at these conditions without the assistance of forced ventilation and without any other noticeable path open to the atmosphere. At a depth of one chord length, the foil appeared to be hyperventilating with a direct path of air movement from the atmosphere to the cavity. Natural ventilation of the foil through the strut wedges was not readily apparent at other conditions or angles of attack, depths and speeds, although pressure data from the trailing-edge transducer indicate that in some of these cases air was reaching that portion of the foil.

During forced ventilation of the foil, it was noted that there existed a lower limit to the quantity of air flow required to form a fully developed cavity, (i.e., one which was clearly distinguishable and at least several chord lengths in size) below which minimum the air simply streamed from the ports. Transition to a cavity flow, which was in some cases abrupt, occurred only when more than this minimum air flow was provided. In addition, the cavity pressure quickly became atmospheric or very nearly atmospheric with a slight

increase in air flow rate, and remained so in spite of any further increase in the air rate. An exception occurred at a speed of 10.3 knots where cavity pressure was increased above atmospheric, but only after a large increase in the air rate.

The inability to increase the cavity pressure above atmospheric during force ventilated flow can be attributed to two factors. In some instances forced ventilation triggered hyperventilation and air escaped directly into the atmosphere. In most other instances, however, it appears that air was lost due to the strut wedges. This latter conclusion is based upon measurements showing that higher than atmospheric pressures were obtained for comparable air rates using a strut without wedges.

MEAN CAVITATION NUMBER

The cavitation number based upon cavity pressure provides, in a general sense, the clearest indication of the behavior of the hydrofoil during these experiments. Other parameters, such as mean lift and drag coefficients, can be directly related to the mean cavitation number. The variation of the mean cavitation number with ventilation index, for example, is reflected in a corresponding variation in mean lift and drag. Consequently, a detailed examination of the cavitation number provides useful insight into the behavior of other experimentally measured parameters.

Figure 4 presents the variation of the cavitation number with ventilation index from experiments in calm water. A limited amount of these data was obtained for comparison with previously reported data for

this foil[1] and to provide a reference base for the results obtained in waves. As shown in Figure 4a, at an angle of attack of 5 degrees the cavitation number for the two speeds tested (10.3 and 20.7 knots), varies with air flow rate only at 10.3 knots. At this speed, the cavity pressure, which is initially atmospheric, is gradually increased by increasing the flow rate or ventilation index at the 3-chord depth. This is reflected in the figure by a decrease in the cavitation number. The cavity pressure at both depths examined at the 20.7 knot speed remained atmospheric regardless of flow rate. A cavity on the upper surface of the flow was not visible during experiments at this angle of attack, but such a cavity may have existed and been too thin to observer. The data indicate that, at the very least, an air path was open between the atmosphere and the pressure gage located on the backside of the foil.

A somewhat more definitive picture emerges from the calm water results obtained at an angle of attack of 10 degrees shown in Figure 4b. At a speed of 10.3 knots, natural ventilation occurred due to the strut wedges and resulted in the development of a clearly visible cavity. At other conditions, a relatively small amount of air was required to initiate a cavity which appeared to develop rather abruptly. The cavity pressure quickly became atmospheric and remained so in spite of the injection of large quantities of air. An exception occurred again for the 3 chord depth at 10.3 knots where an increase in cavity pressure was realized, but only after a large increase in ventilation index.

Failure to increase the cavity pressure above atmospheric indicates that the cavity was in some manner open to the atmosphere through which most of the air escaped. In some instances it was observed that hyperventilation could be initiated by force ventilation particularly at a depth of one chord. This was noted by the persistence of the cavity long after termination of the air supply to the foil. Air supplied to the foil during hyperventilated flow would obviously escape to the atmosphere. In most cases, however, it appears as though the air escaped by means of the wedges. Data to be presented later show that cavity pressure higher than atmospheric can be obtained at comparable flow rates by using a strut without wedges.

The calm water results for an angle of attack of 14 degrees, presented in Figure 4c, show a smoother transition of the cavitation number with ventilation index than previous results. Also, cavity pressures greater than atmospheric were obtained by forced ventilation, although it is apparent that air had excaped via the strut wedges. Changing the angle of attack of the foil required changing the strut angle and this may have reduced the effectiveness of the air path created by the wedges.

The variation of the mean cavitation number with ventilation index in regular waves is roughly the same as in calm water, with only slight modification. These data are presented in Figure 5. Each graph shows the variation of the mean cavitation number with ventilation index at a specific angle of attack and foil depth for various combinations of wave length and forward speed. The wave amplitude (single) was 3 inches in all cases shown. Curves have been drawn through the data spots to assist in

distinguishing general trends, and these curves may not necessarily precisely reflect the behavior of the cavitation number at low ventilation indices.

As in the calm water experiments, air supplied to the upper surface of the foil escaped either via the wedges or by hyper-ventilation. Thus, a build-up of cavity pressure much above atmospheric could not be realized by forced ventilation. This is best illustrated in Figures 5(a), 5(b), and 5(c) which show data for an angle of attack of 10 degrees at depths of 1, 2, and 3 chord lengths, respectively. In all cases, except at a speed of 10.3 knots, the cavity pressure reaches a plateau at about atmospheric pressure and does not change in spite of large increases in the ventilation index. This is consistent with results obtained in calm water.

The transition from high to low cavitation number, which occurs at a ventilation index of about 0.05 appears to be somewhat unstable and is dependent upon the wave length. In long waves (λ = 30 and 40 feet), the transition is generally smoother than in calm water, whereas in short waves (λ = 15 feet) the transition and behavior is more nearly the same as in calm water. Occasional departure from this trend may be noted, suggesting some instability in this region. Beyond the transition region, for high ventilation indices, small differences in the mean cavitation number were obtained in the different wave lengths for the same ventilation index, particularly at the lower speeds. There are also differences between the head and following wave results. These differences are not large and no consistent trend is readily apparent.

Some experiments were conducted in regular waves with the wedges removed from the strut and the air path for natural ventilation of the foil eliminated. These results, which were obtained at an angle of attack of 10 degrees and a foil depth of two chord lengths, are shown in Figure 5d. The data show that the cavity pressure, limited to atmospheric pressure with the strut wedges, can be further increased somewhat by forced ventilation without the strut wedges. It may also be observed that the cavitation number for all conditions examined is approximately the same at corresponding values of ventilation index. These results suggest that the air loss during forced ventilation occurred primarily via the strut wedges at the larger foil depths.

MEAN LIFT AND DRAG

Figures 6 and 7 present the experimentally determined mean lift coefficients plotted with respect to the ventilation index. These figures match those previously presented for the mean cavitation number. It is apparent upon examination of these data that the behavior of the mean lift coefficient is consistent with the variation of the mean cavitation number. For this reason, the mean lift coefficients have been replotted with respect to the mean cavitation number and are presented in Figures 8 and 9. These plots have been terminated at a cavitation number near 0.30 to exclude most of those data obtained without a fully developed cavity on the upper surface of the foil.

At an angle of attack of 5 degrees the data show considerable scatter, indicating that the flow conditions were not stable. Consequently, the following comments and conclusions which are based on the data obtained at this angle of attack are not as well supported as are those based on

data obtained at the higher angles of attack. The data show that, within experimental accuracy, the mean lift coefficient for a given angle of attack is a functior of the cavitation number only and virtually independent of wave length, foil speed and depth (for depths of one chord length and greater). Also, the mean lift coefficient in waves is the same as in calm water.

A comparison of the mean lift coefficient obtained during these experiments with those reported in Reference 1 shows excellent agreement.. This is especially noteworthy since in this experiment the cavitation number was computed on the basis of the measured mean cavity pressure, whereas in the referenced data the cavitation number was computed on the basis of the vapor pressure. This indicates that for a given angle of attack, the mean lift coefficient is a function of the mean cavitation number only, irrespective of the cavity pressure. More specifically, the mean lift coefficient is the same for supercavitating or ventilating flow at a given angle of attack and cavitation number provided a fully developed cavity exists on the upper surface of the foil.

Mean drag coefficient data have been plotted with respect to mean cavitation number as was done for the lift coefficient and are presented in Figures 10 and 11. The mean drag coefficient data, like the mean lift coefficient data, also appears to be independent of wave length, foil speed, and foil depth. Any differences which may exist between results obtained in the different wave lengths are too small to distinguish from experimental scatter (which is also very small). More significantly, the mean drag in head waves is higher, and in following waves lower, than that obtained in calm water.

In summary, steady state lift and mean lift in waves; are the same however, mean drag in waves includes an additional contribution due to the waves.

OSCILLATORY LIFT AND DRAG

Oscillatory lift and drag data are plotted in nondimensional form with respect to ventilation index in Figures 12 and 13. Curves are drawn through the data points only to assist in distinguishing general trends and should not be interpreted as describing the precise behavior of the data especially at low values of ventilation index.

The oscillatory lift coefficient data obtained at an angle of attack of 5 degrees shown in Figures 12(b) and 12(c), was constant for depths of 2 and 3 chord lengths. At a depth of one chord length, a different constant was obtained for different speeds. These results are consistent with observations at this angle of attack that the flow was essentially wetted for all speeds examined and that air injection had no major influence on foil behavior.

The oscillatory lift data obtained at angles of attack of 10 degrees and greater follow a pattern which is very much in accordance with the variation in mean cavitation number and mean lift in waves. Consider the data, for example, obtained at an angle of attack of 10 degrees and a depth of 2 chord lengths, which is shown in Figure 12(e). At low values of the ventilation index, where the lift slope is the steepest, the oscillatory lift coefficient is appropriately the highest. Increasing the

the ventilation index results in a rapid decrease in the oscillatory lift coefficients to some constant similar to the behavior of the mean cavitation number. Paradoxically, at a speed of 10.3 knots, the oscillatory lift increases at very high ventilation indices, whereas the mean cavitation number and mean lift actually decreased.

The effect of wave length on the oscillatory lift within the range of the experimental parameter examined, is not very noticeable, although some differences probably do exist as expected from quasi-steady considerations. The effect of speed is more apparent since it alters the mean cavitation number which directly influences the oscillatory lift.

The behavior of the oscillatory drag coefficient data shown in Figure 12 is roughly the same as the oscillatory lift. At some conditions, the effect of wave length was more noticeable than at others. For example, at an angle of attack of 14 degrees and a depth of one chord length, shown in Figure 13(g), large differences were obtained between wave lengths at a speed of 10.3 knots. Also, in some instances, wave amplitude had a significant effect on the mean drag coefficient as shown in Figure 12(f) for an angle of attack of 10 degrees and 3 chord depths at a speed of 10.3 knots. In general, the effects of wave length and amplitude appear to be more pronounced for the oscillatory drag than for the oscillatory lift.

SUMMARY AND CONCLUSIONS

The flow behavior of the strut foil system was complicated by the combining of the two different methods of ventilation, i.e. natural ventilation by use of strut wedges and forced ventilation by blowing air through ports in the upper surface of the foil. Forced ventilation resulted in the development of a full cavity on the upper surface of the foil except at an angle of attack of 5 degrees (which was the lowest examined). The mean cavitation number was lowered by increasing air flow until the cavity pressure reached atmospheric pressure. Further increase in air flow did not result in any further decrease in the cavitation numbers at comparable conditions, indicating that air escaped past the strut wedges when in use. Also, in some instances forced ventilation triggered hyperventilation and air escaped through the rear of the cavity.

Once a full cavity was developed the mean lift coefficient was dependent only upon the mean cavitation number and independent of wave length, foil speed and foil depth within the range that was examined, and the results in calm water and waves were the same. Excellent agreement was obtained in comparing these results for ventilated flow on the basis of cavitation number with those previously reported for supercavitating flow conditions. This is especially significant since the cavitation number for the supercavitating results was computed on the basis of vapor pressure. The mean drag data also appears to be a function of cavitation number (once a full cavity is developed); however, the mean drag in head waves is higher and in following waves lower than that in calm water.

The oscillatory lift and drag of the foil, in general, followed the same behavior as the mean cavitation number and mean lift and drag. The oscillatory lift was the highest at low air flow rates where the flow was essentially wetted or partially cavitating and lift curve slope the steepest. As the air flow was increased, the oscillatory lift decreased following the decrease in the mean cavitation number. The effect of wave length on the oscillatory lift was too small for the wave lengths examined to infer any general behavior of trend. The effect of wave length and height on the oscillatory drag was in some instances more noticeable than in others; but no consistent trend was readily apparent.

In these experiments the speeds selected were based upon Froude scaling using a 1/15 scaled model. Scaling for ventilated flows, and in particular those which combine both natural and forced ventilation, is not completely understood, and extrapolation of the experimental results in this report to the prototype should not be attempted without due caution.

ACKNOWLEDGMENTS

The authors wish to express their appreciation to Messrs. M. Pemberton, M. Davis, and B. Peters for their contributions to the testing on the carriage and the computer programming for the Interdata System. Special appreciation is due to Drs. Y. Shen and M. Martin for the guidance and direction in establishing the test program.

REFERENCES

1. Dobay, G.F., "Influence of Scale Ratio, Aspect Ratio and Planform on the Performance of Supercavitating Hydrofoils," NSRDC Report 2390, August 1967

2. Ficken, Jr., N.L. and Dobay, G.F., "Experimental Determination of the Forces on Supercavitating Hydrofoils with Internal Ventilation," NSRDC Report 1676, January 1963.

APPENDIX

DATA REDUCTION

Processing of the data was accomplished primarily by utilization of the Interdata computer system during the experiment on the carriage. The following information was obtained in engineering units for each experimental condition:

- mean
- root mean square (RMS)
- standard deviation
- single amplitude

for each of the following channels

- forward lift gage
- aft lift gage
- lift summation
- forward drag gage
- aft drag gage
- drag summation
- foil depth
- pressure behind the foil's trailing edge
- carriage speed
- wave amplitude

Furthermore, a number of nondimensionalized quantities were computed such as:

$$\text{Mean lift coefficient } \overline{C}_L = \frac{\overline{L}}{qS} \qquad (1)$$

Amplitude of oscillatory lift coefficient	$\Delta C_L = \frac{\Delta L}{qS}$	(2)
Mean drag coefficient	$\overline{C}_D = \frac{\overline{D}_m}{qS} - 0.021d$	(3)
Amplitude of oscillatory drag coefficient	$\Delta C_D = \frac{D_m}{qS}$	(4)
Lift/Drag ratio	$\overline{L/D}_m$	(5)
Cavitation number	$\sigma_c = \frac{p_\infty - p_c}{q}$	(6)

The mean drag coefficient $\overline{C}_D$ as presented in this report applies to the hydrofoil only, i.e., the drag component due to the strut and given by the second terms in equation (4) was subtracted from the total measured drag coefficient as given by the first term. The strut drag component was obtained from experimental data and with reference to previous strut drag determinations.[2] All oscillatory quantities as analyzed by the Interdata computer system are based on the RMS of the measured signal.

Additional computations were obtained after the conclusion of the test program by a reanalysis of the digital magnetic tape on the Interdata. The most significant nondimensional quantities also based on the signal's RMS value were:

$$\frac{\Delta C_L}{\Delta \alpha} \qquad (7)$$

and

$$\frac{\Delta C_D}{\Delta \alpha} \qquad (8)$$

where $\Delta\alpha$ = change in angle of attack due to the orbital velocity of water particles in waves

$$\Delta\alpha = \frac{\zeta\omega_o e^{-k}}{V} \qquad (9)$$

From the forced ventilation volumetric air-flow rate, corrected to atmospheric pressure Q, hydrofoil speed V, and foil angle of attack, the nondimensional ratio designated ventilation index K_v was defined as

$$K_v = \frac{Q}{VA_p}$$

where A_p = projected area of the foil perpendicular to the direction of carriage velocity

$$A_p = A_t + S \sin (\alpha - 5.0^o)$$

A_t = area of hydrofoil trailing edge surface, 0.0390 ft^2.

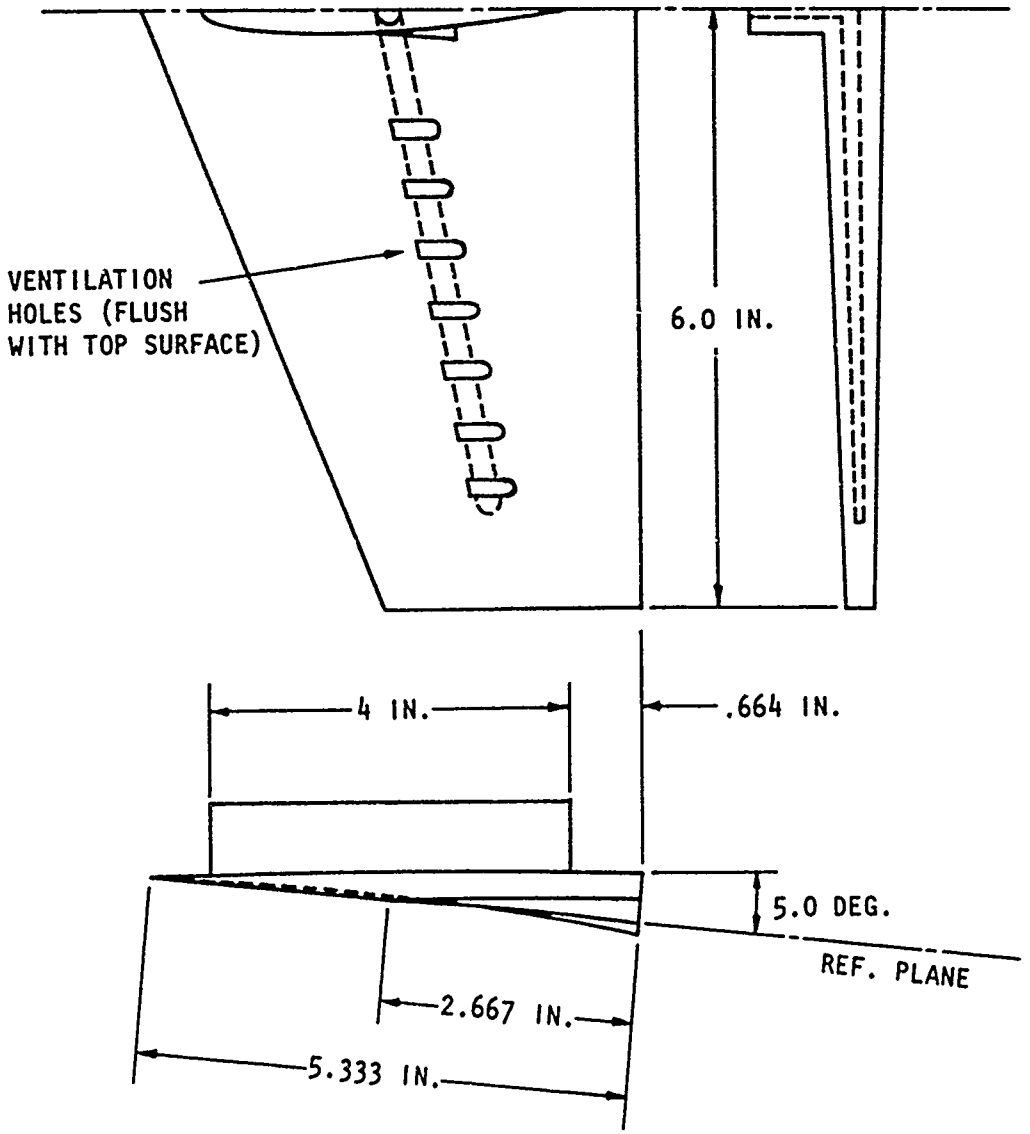

Figure 1 - Hydrofoil H47

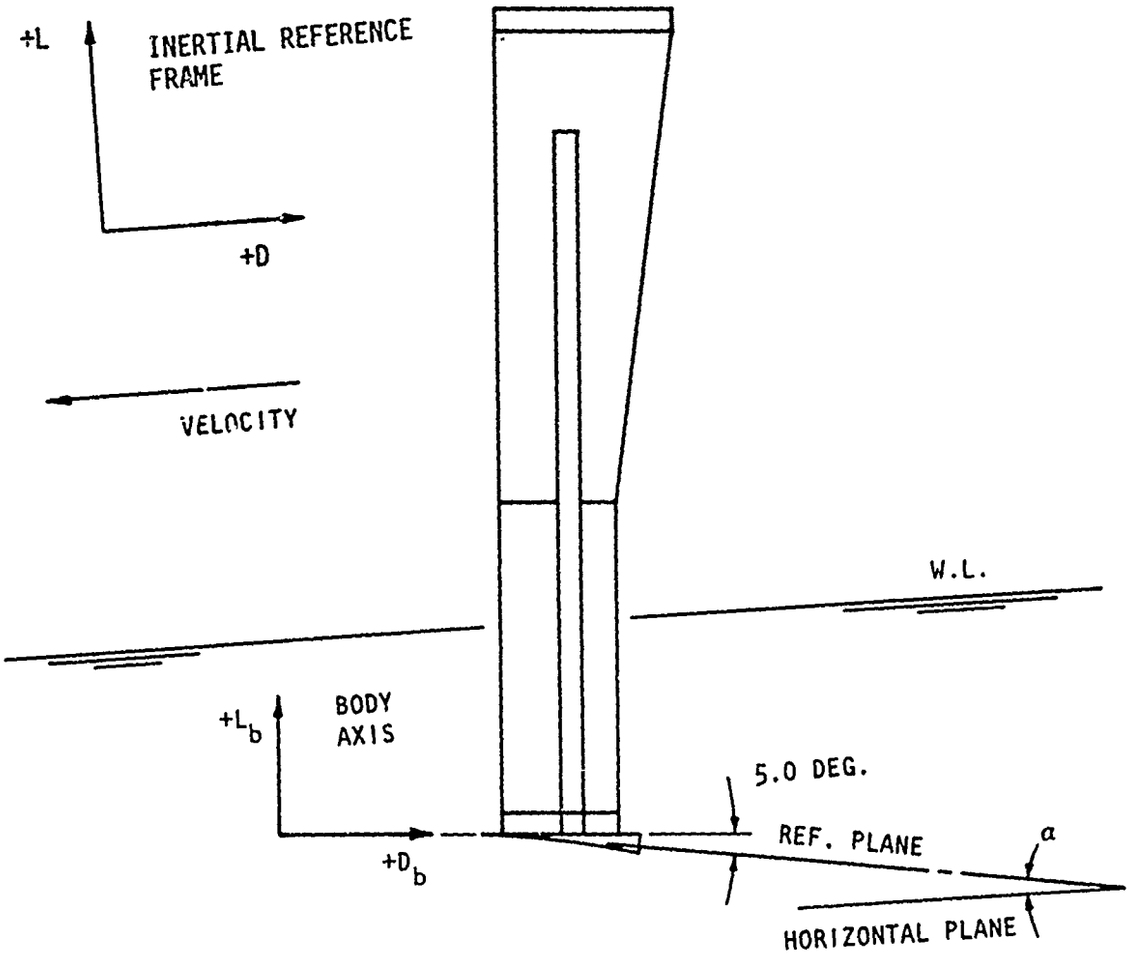

Figure 2 - Hydrofoil-Strut Orientation with Coordinate Axes

HYDROFOIL TOWING STRUT
STRUT SECTION OFFSETS
(MODIFIED NACA 66, 1-0120)

X/C	Y/C
0.0050	0.00900
0.0075	0.01083
0.0125	0.01343
0.025	0.01803
0.050	0.02482
0.075	0.03019
0.10	0.03482
0.15	0.04214
0.20	0.04779
0.25	0.05218
0.30	0.05550
0.35	0.05786
0.40	0.05934
0.45	0.05998
* 0.50	0.05972
0.55	0.06457
0.60	0.06941
0.65	0.07426
0.70	0.07910
0.75	0.03789
0.80	0.02964
0.85	0.02098
0.90	0.01244
0.95	0.00477
1.00	0

* MODIFICATION EXTENDS
FROM X/C = 0.500
TO X/C = 0.700
WITH THE GIVEN OFFSETS APPLICABLE ONLY
TO THE LOWER 10-INCH LONG CYLINDRICAL
STRUT PORTION

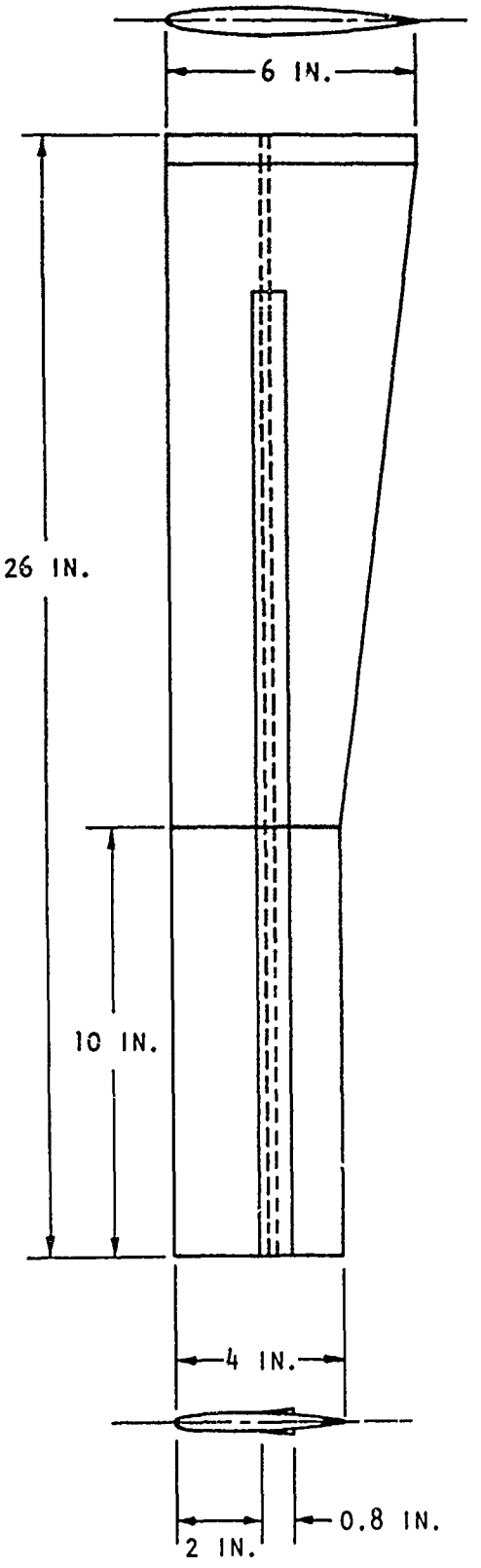

Figure 3 - Hydrofoil Strut Offsets and Geometry

Figure 4 - Variation of Cavitation Number with Ventilation Index in Calm Water.

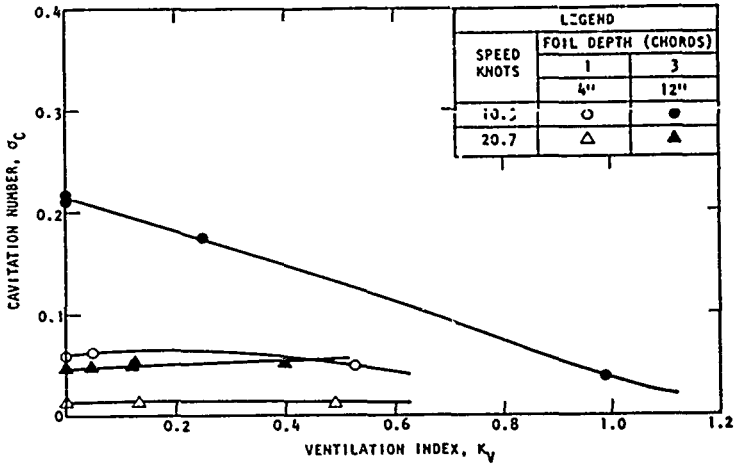

Figure 4a - 5.0 Degrees Angle of Attack.

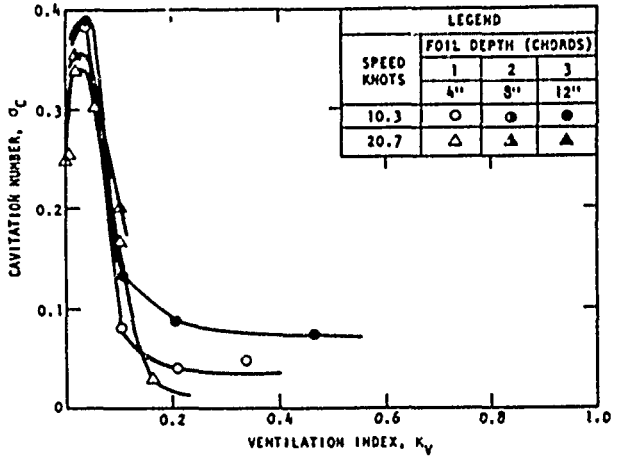

Figure 4c - 14.0 Degrees Angle of Attack.

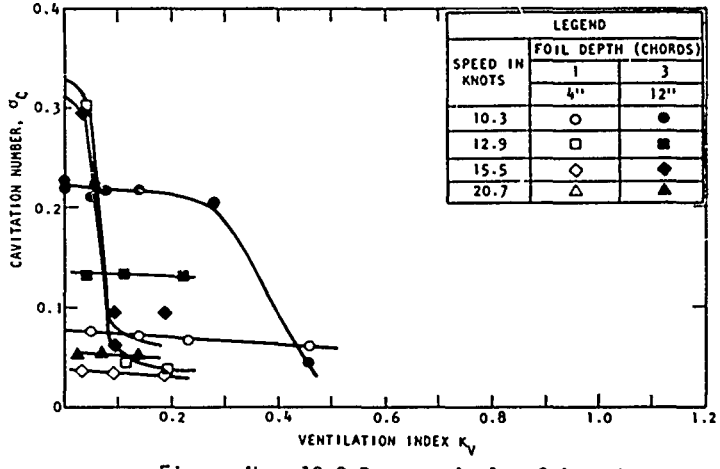

Figure 4b - 10.0 Degrees Angle of Attack.

Figure 5 - Variation of Mean Cavitation Number with Ventilation Index in Regular Waves.

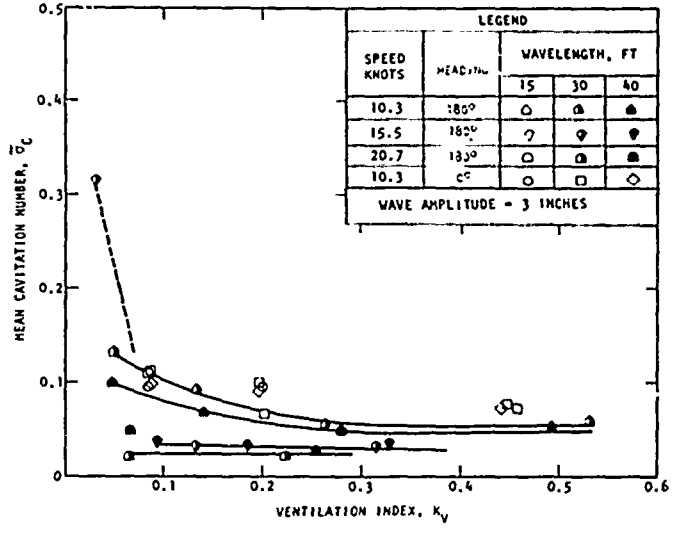

Figure 5a - 10.0 Degrees Angle of Attack, 1 Chord Depth.

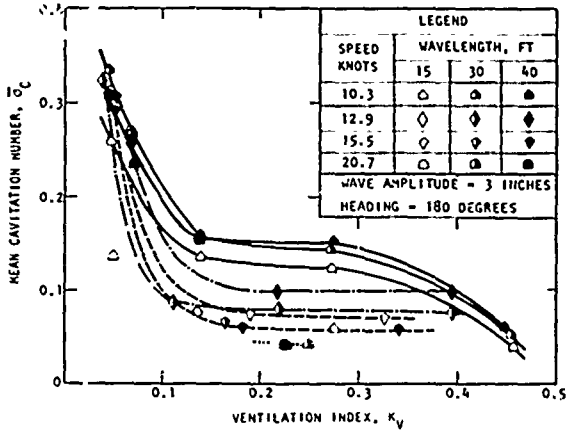

Figure 5b - 10.0 Degrees Angle of Attack, 2 Chords Depth.

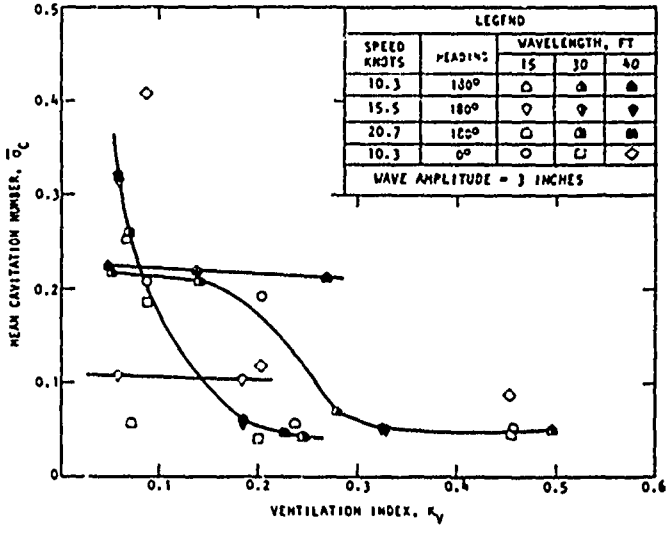

Figure 5c - 10.0 Degrees Angle of Attack, 3 Chords Depth.

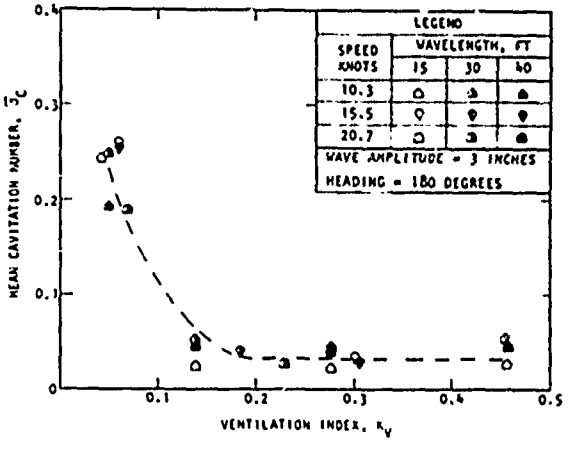

Figure 5d - 10.0 Degrees Angle of Attack, 2 Chords Depth Without Strut Wedges.

Figure 5 - Continued

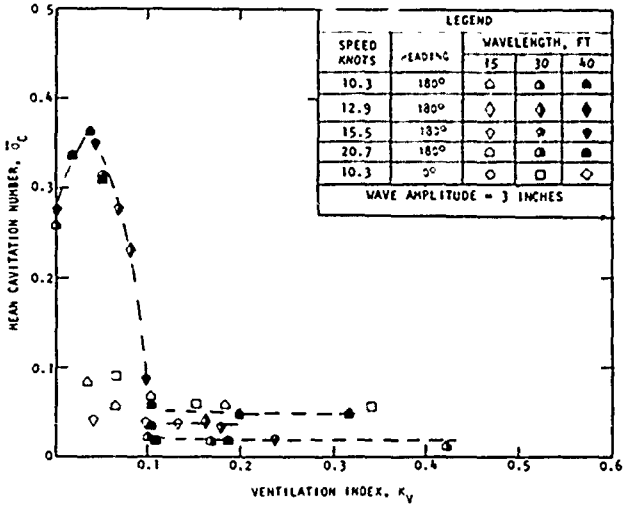

Figure 5e - 14.0 Degrees Angle of Attack, 1 Chord Depth.

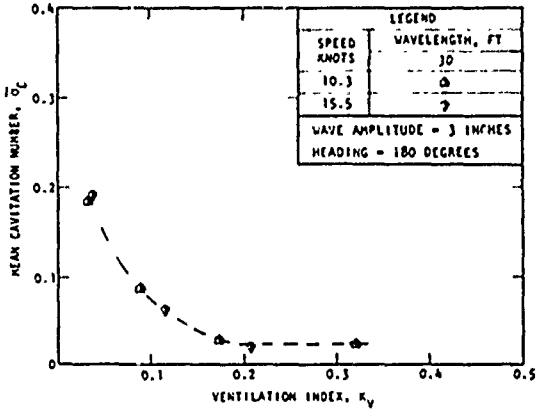

Figure 5g - 17.0 Degrees Angle of Attack, 1 Chord Depth.

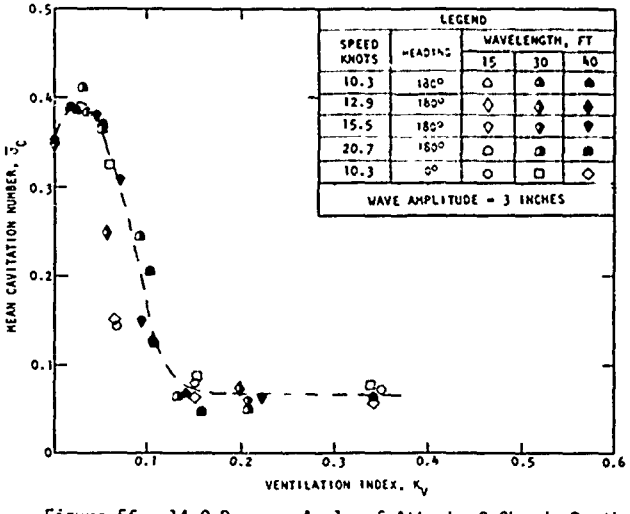

Figure 5f - 14.0 Degrees Angle of Attack, 2 Chords Depth.

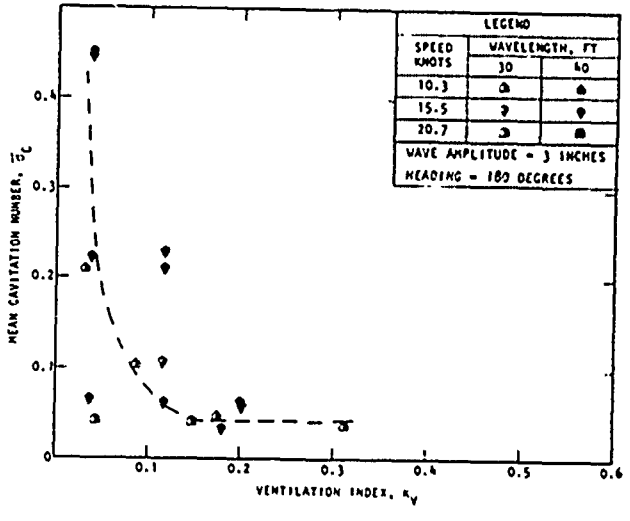

Figure 5h - 17.0 Degrees Angle of Attack, 2 Chords Depth.

Figure 6 - Variation of Lift Coefficient with Ventilation Index in Calm Water.

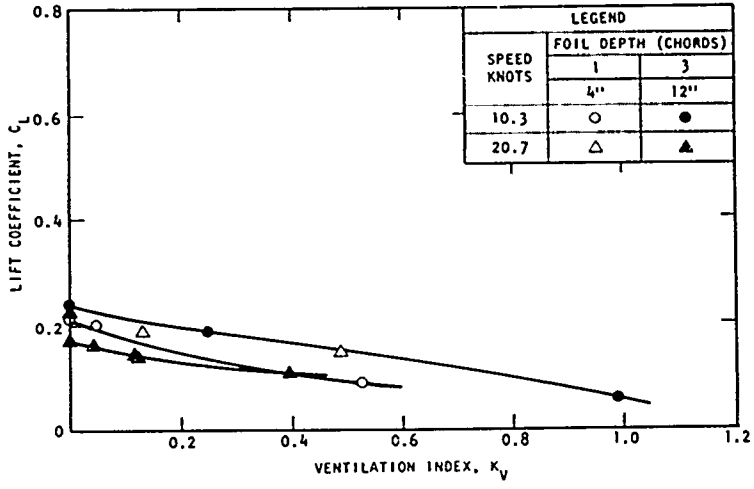

Figure 6a - 5.0 Degrees Angle of Attack.

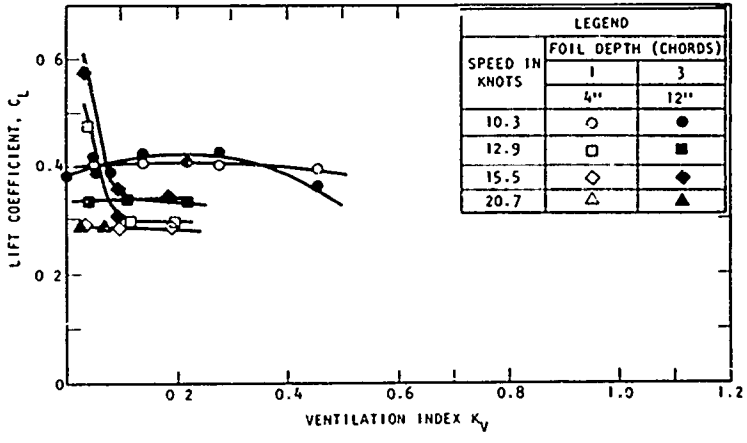

Figure 6b - 10.0 Degrees Angle of Attack.

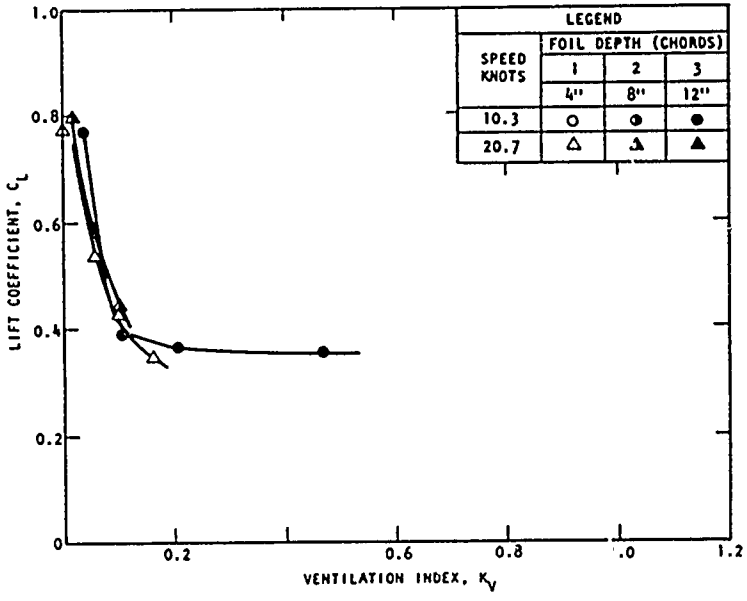

Figure 6c - 14.0 Degrees Angle of Attack.

Figure 7 - Variation of Mean Lift Coefficient with Ventilation Index in Regular Waves.

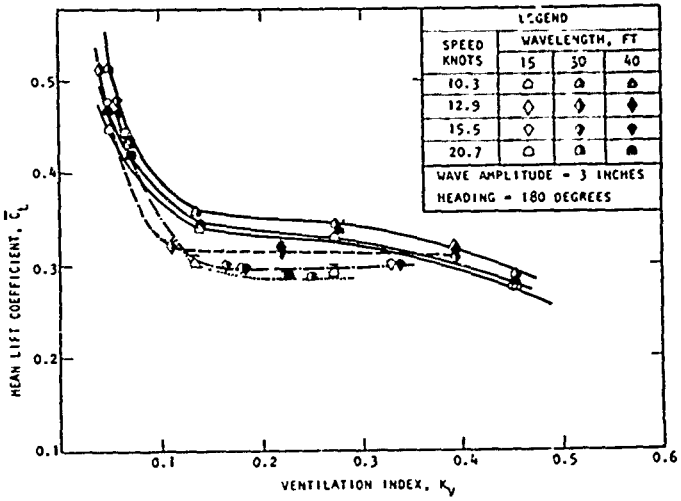

Figure 7a - 10.0 Degrees Angle of Attack, 2 Chords Depth.

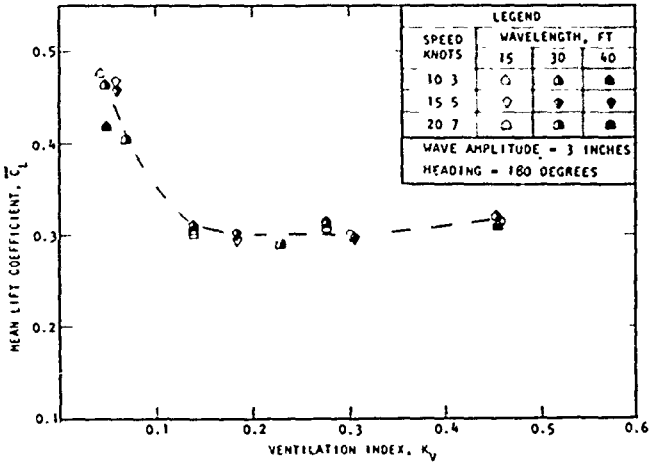

Figure 7b - 10.0 Degrees Angle of Attack, 2 Chords Depth Without Strut Wedges.

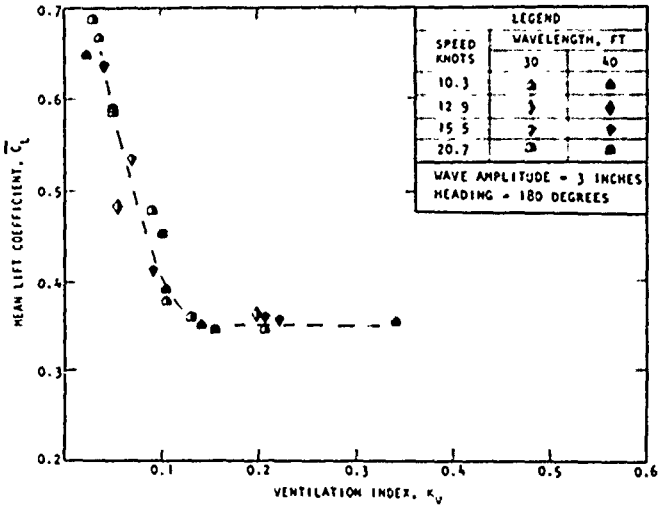

Figure 7c - 14.0 Degrees Angle of Attack, 2 Chords Depth.

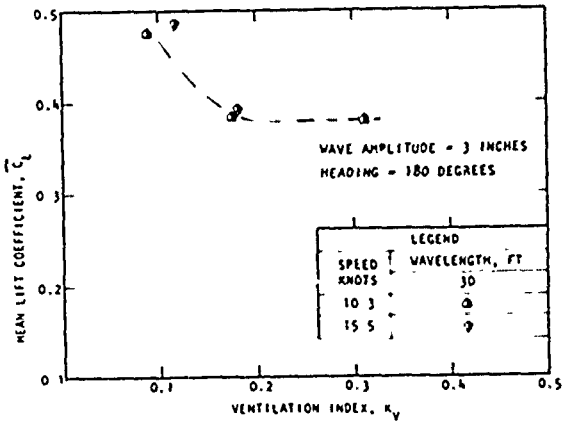

Figure 7d - 17.0 Degrees Angle of Attack, 2 Chords Depth.

Figure 8 - Variation of Lift Coefficient with Cavitation Number in Calm Water.

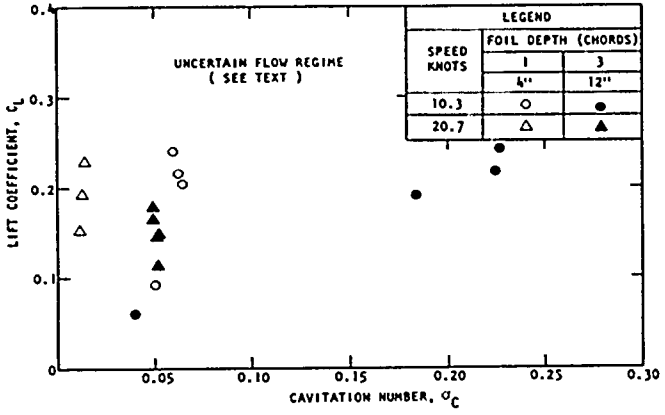

Figure 8a - 5.0 Degrees Angle of Attack.

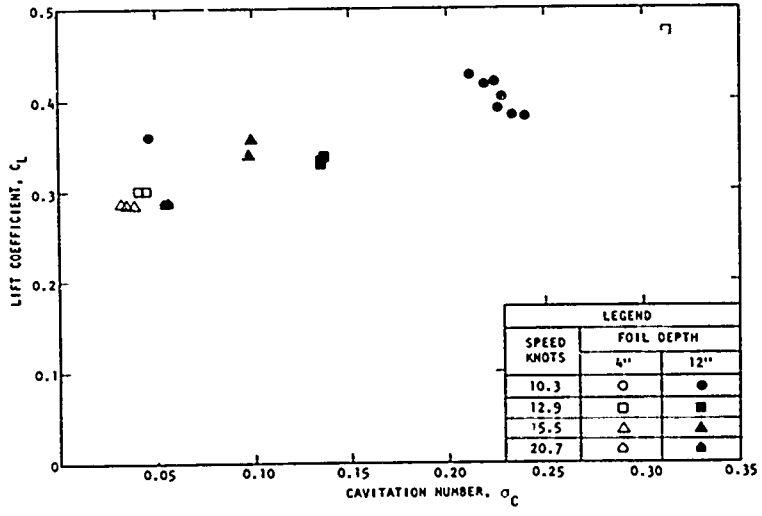

Figure 8b - 10.0 Degrees Angle of Attack.

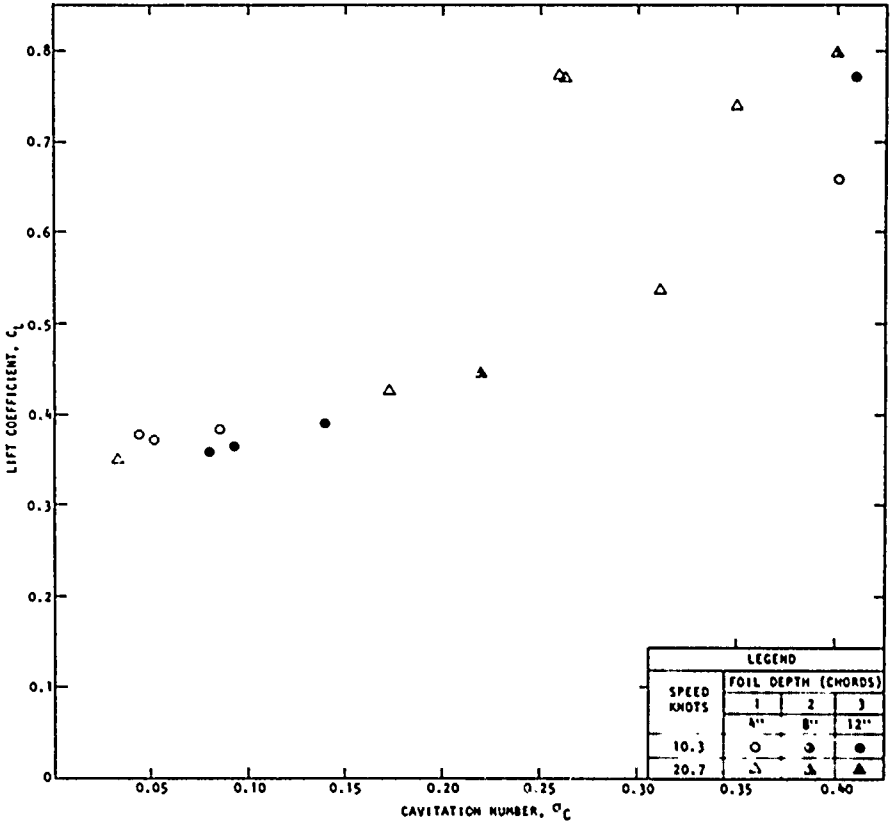

Figure 8c - 14.0 Degrees Angle of Attack.

Figure 9 - Variation of Mean Lift Coefficient with Mean Cavitation Number in Regular Waves.

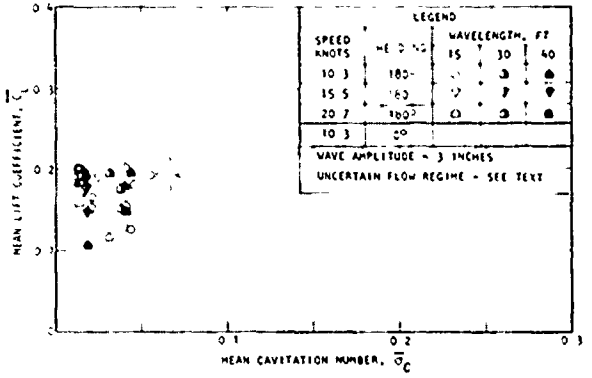

Figure 9a - 5.0 Degrees Angle of Attack, 1 Chord Depth.

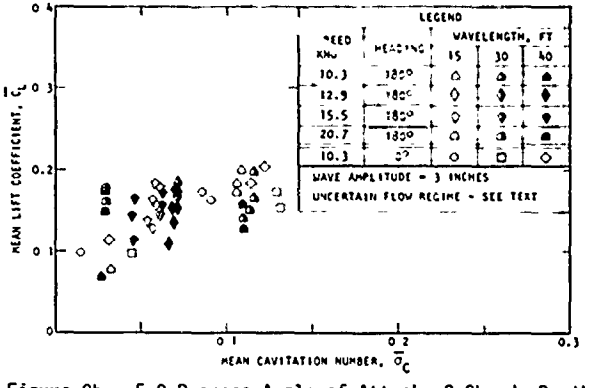

Figure 9b - 5.0 Degrees Angle of Attack, 2 Chords Depth.

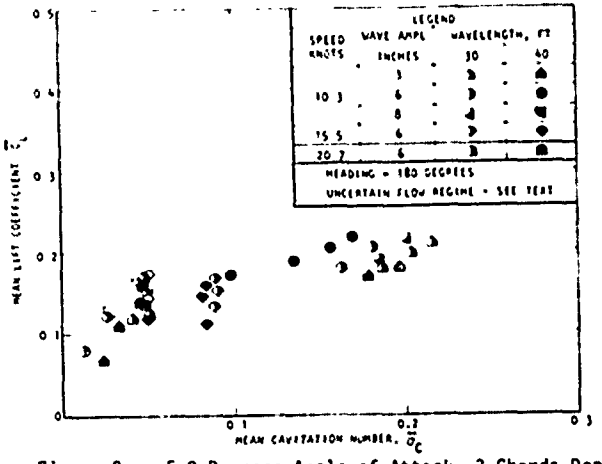

Figure 9c - 5.0 Degrees Angle of Attack, 3 Chords Depth.

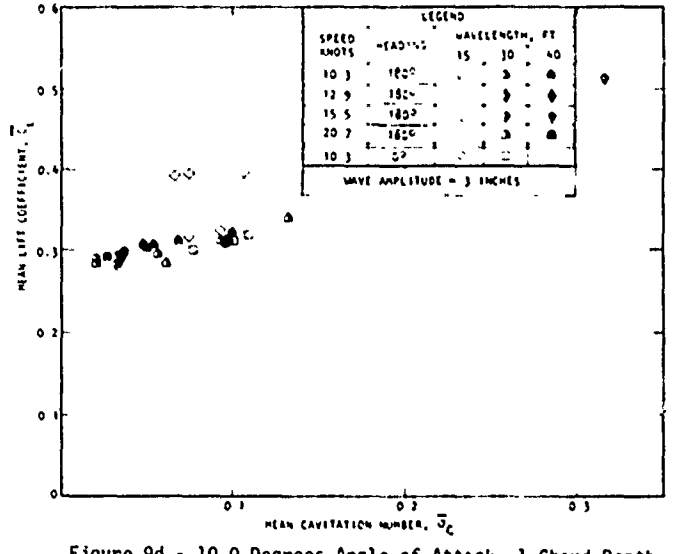

Figure 9d - 10.0 Degrees Angle of Attack, 1 Chord Depth.

Figure 9 - Continued

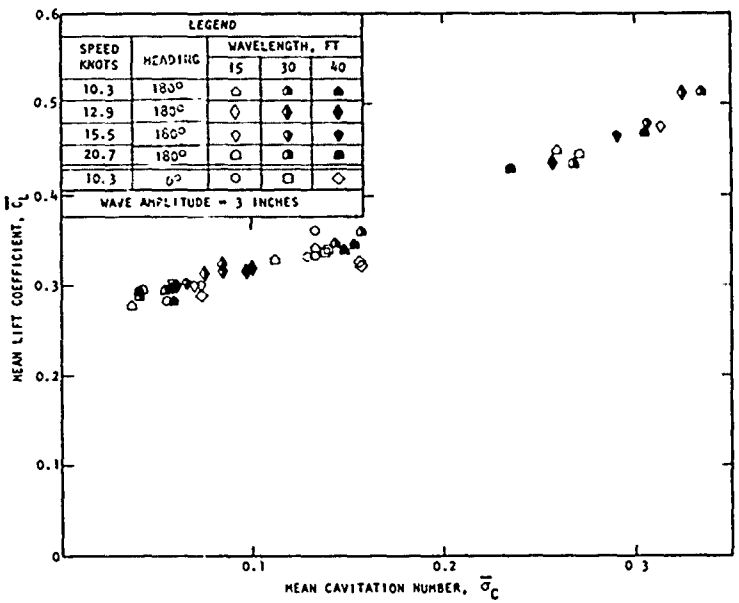

Figure 9e - 10.0 Degrees Angle of Attack, 2 Chords Depth.

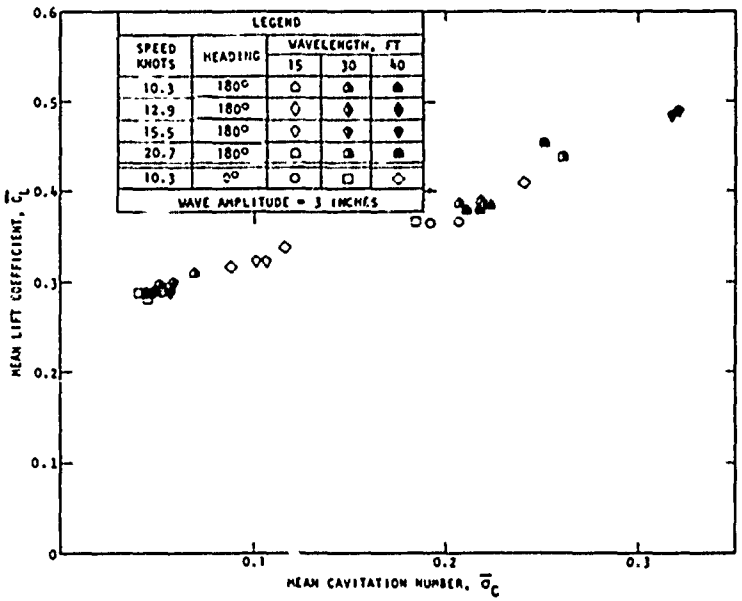

Figure 9f - 10.0 Degrees Angle of Attack, 3 Chords Depth.

Figure 9 - Continued

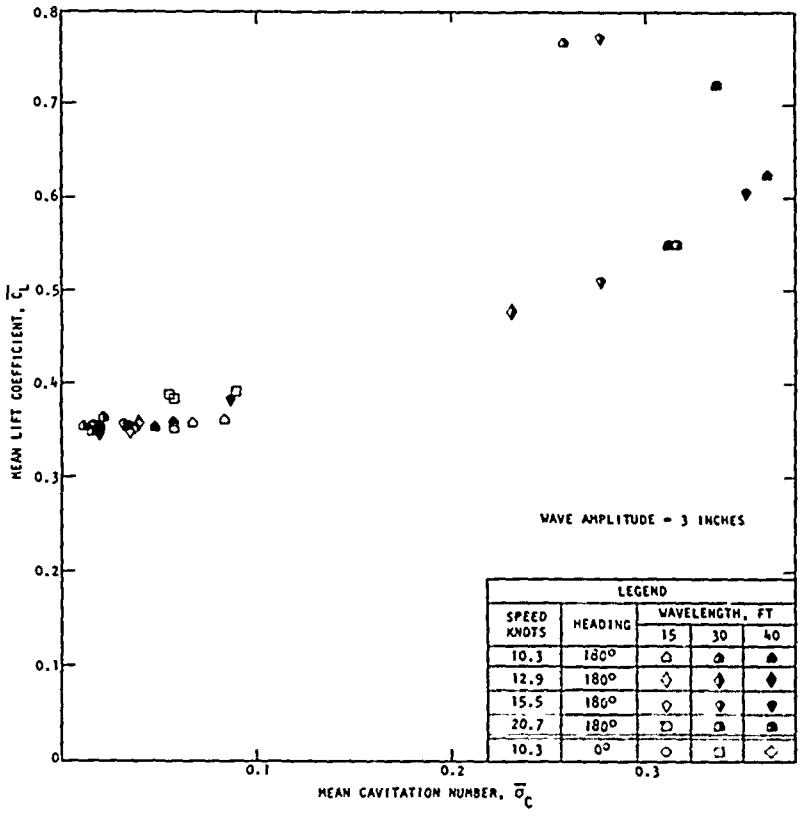

Figure 9g - 14.0 Degrees Angle of Attack, 1 Chord Depth.

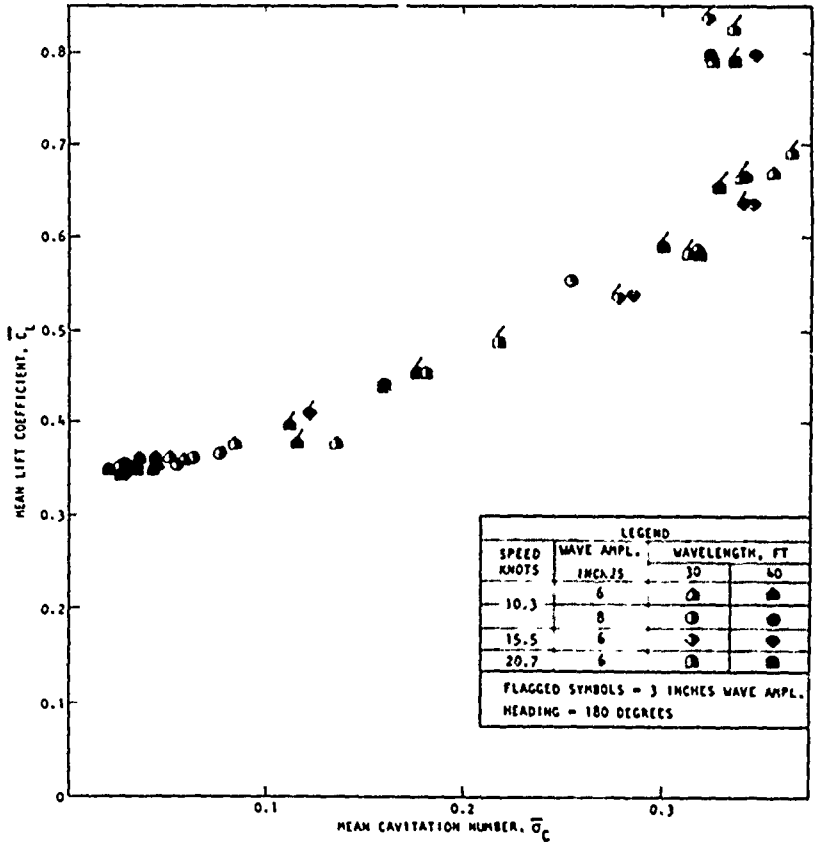

Figure 9h - 14.0 Degrees Angle of Attack, 2 Chords Depth.

Figure 9 - Continued

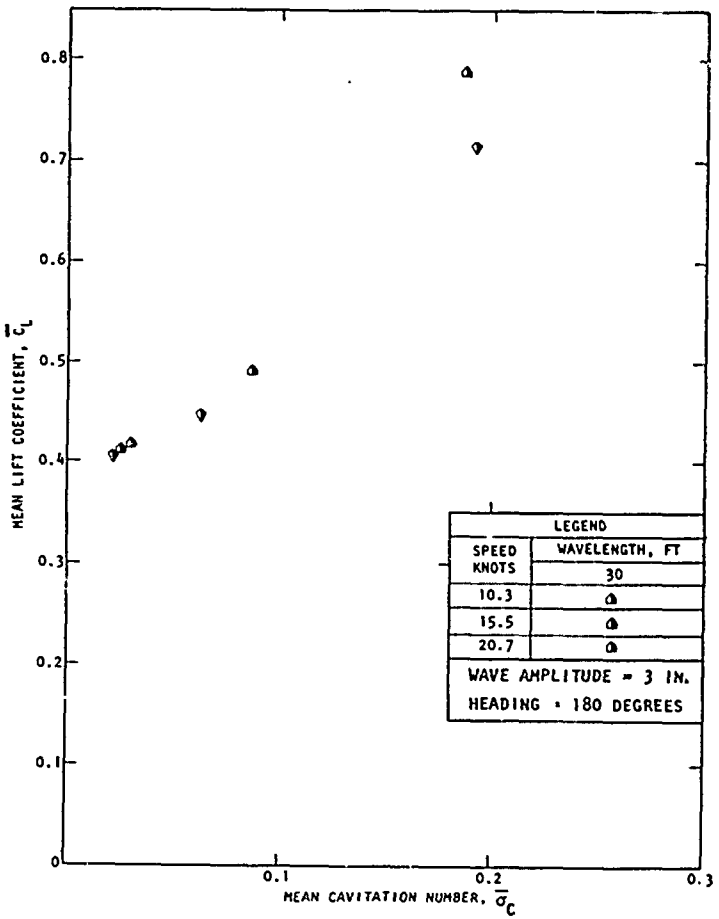

Figure 9i - 17.0 Degrees Angle of Attack, 1 Chord Depth.

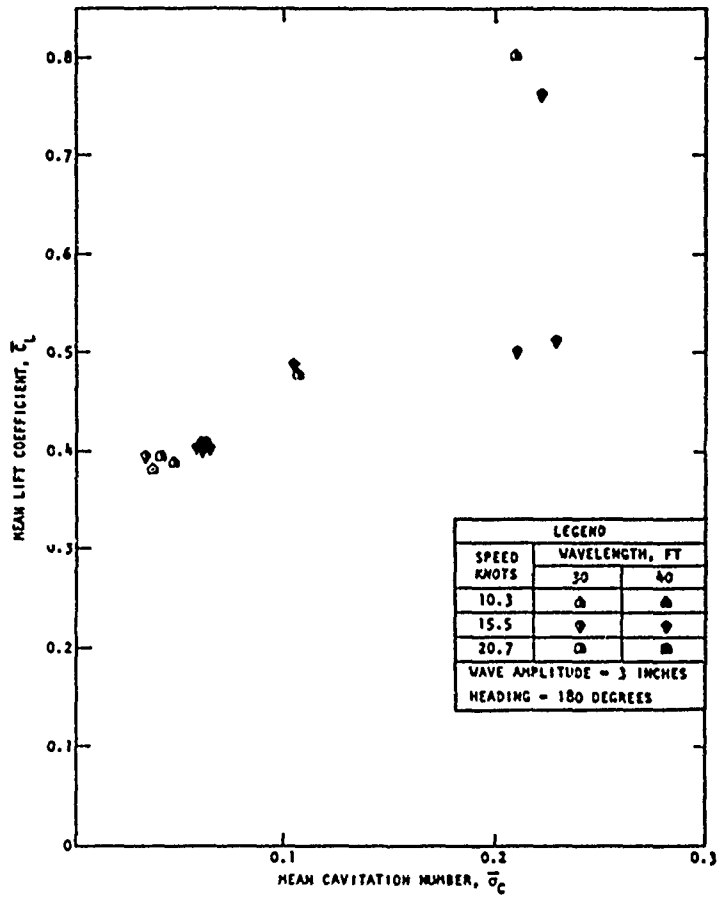

Figure 9j - 17.0 Degrees Angle of Attack, 2 Chords Depth.

Figure 10 - Variation of Drag Coefficient with Cavitation Number in Calm Water.

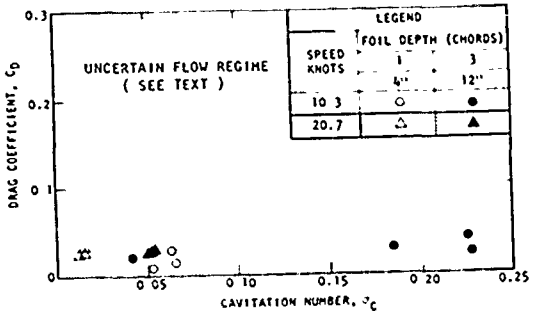

Figure 10a - 5.0 Degrees Angle of Attack.

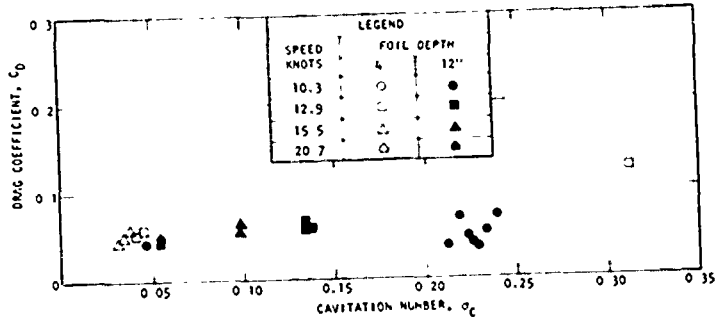

Figure 10b - 10.0 Degrees Angle of Attack.

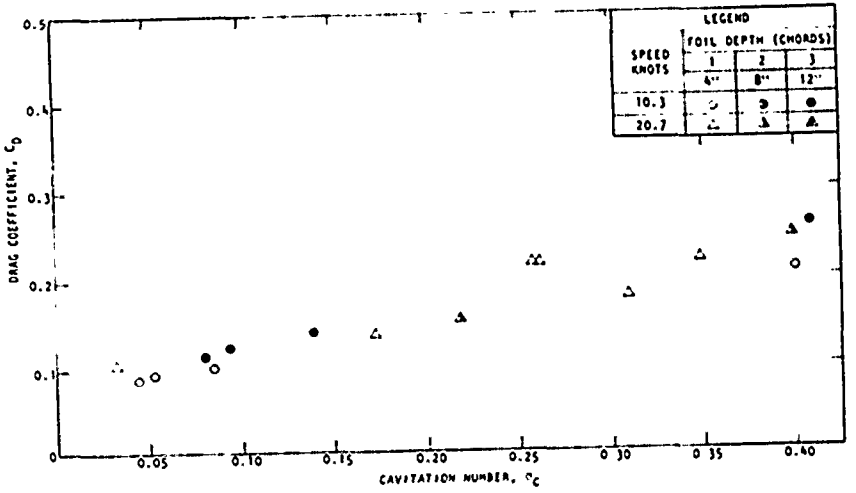

Figure 10c - 14.0 Degrees Angle of Attack.

Figure 11 - Variation of Mean Drag Coefficient with Mean Cavitation Number in Regular Waves.

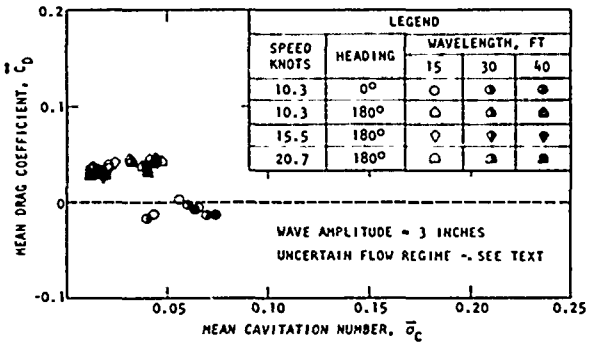

Figure 11a - 5.0 Degrees Angle of Attack, 1 Chord Depth.

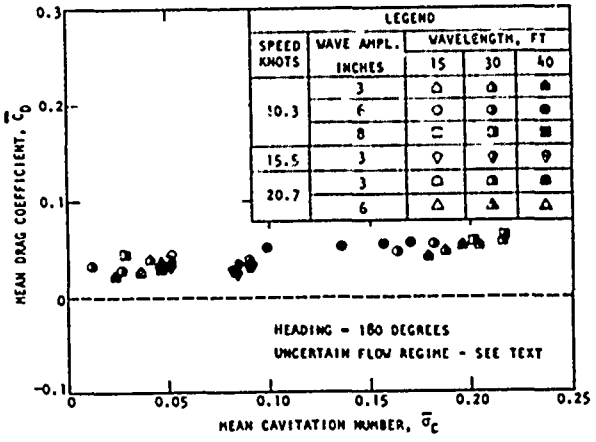

Figure 11c - 5.0 Degrees Angle of Attack, 3 Chords Depth.

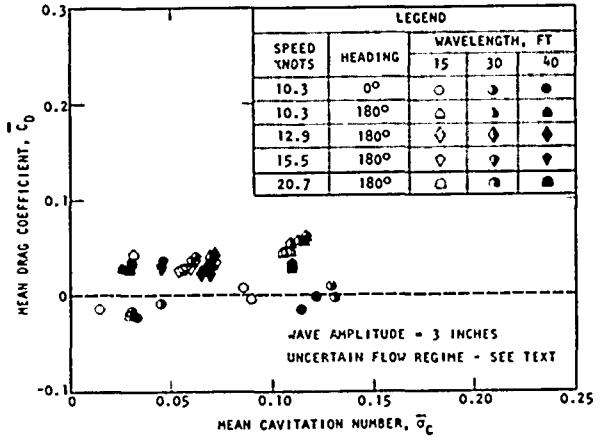

Figure 11b - 5.0 Degrees Angle of Attack, 2 Chords Depth.

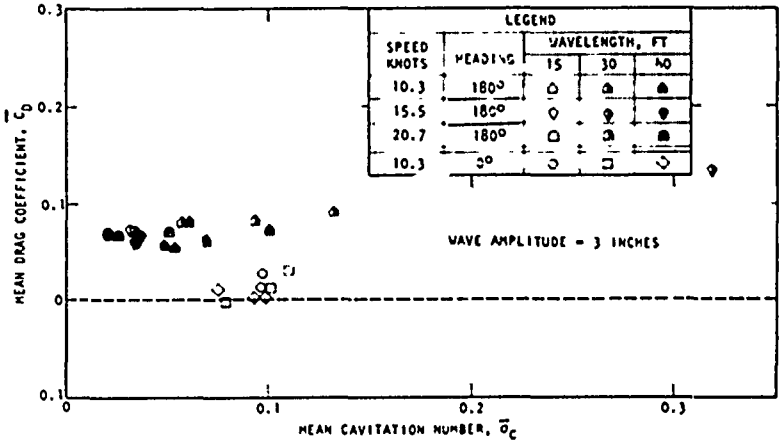

Figure 11d - 10.0 Degrees Angle of Attack, 1 Chord Depth.

Figure 11 - Continued

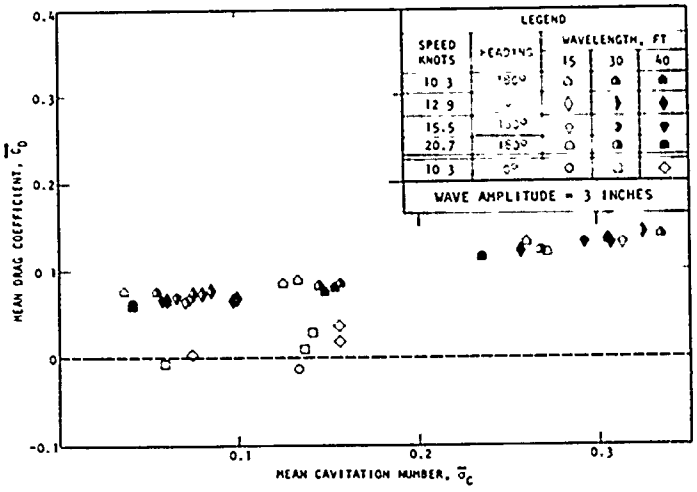

Figure 11e - 10.0 Degrees Angle of Attack, 2 Chords Depth.

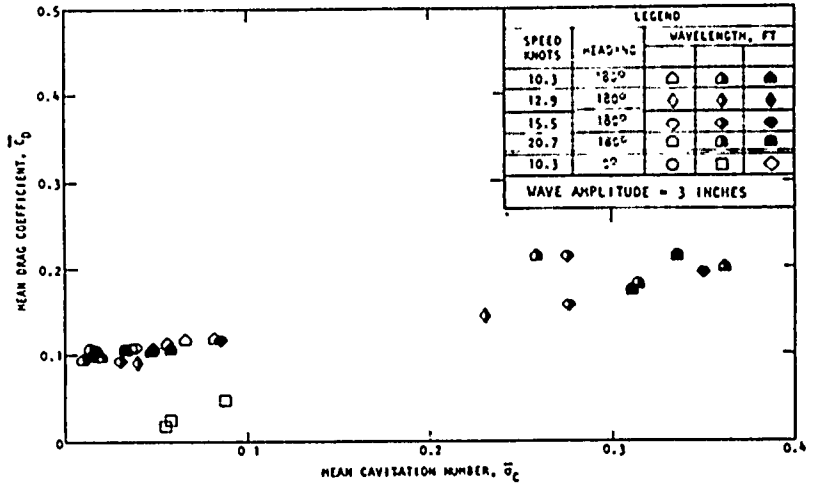

Figure 11g - 14.0 Degrees Angle of Attack, 1 Chord Depth.

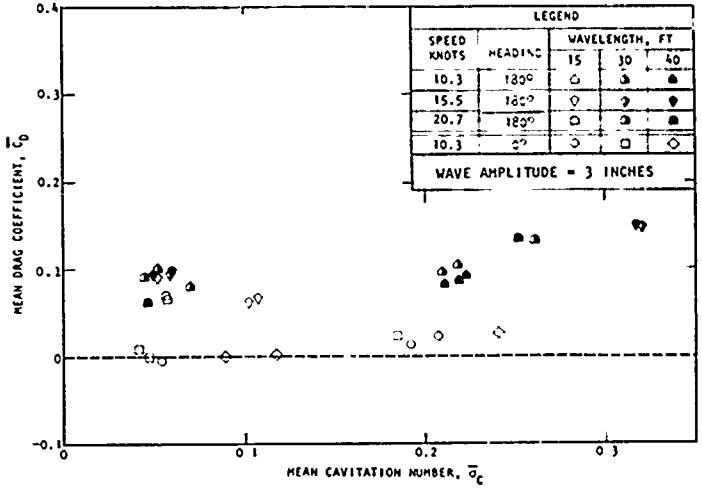

Figure 11f - 10.0 Degrees Angle of Attack, 3 Chords Depth.

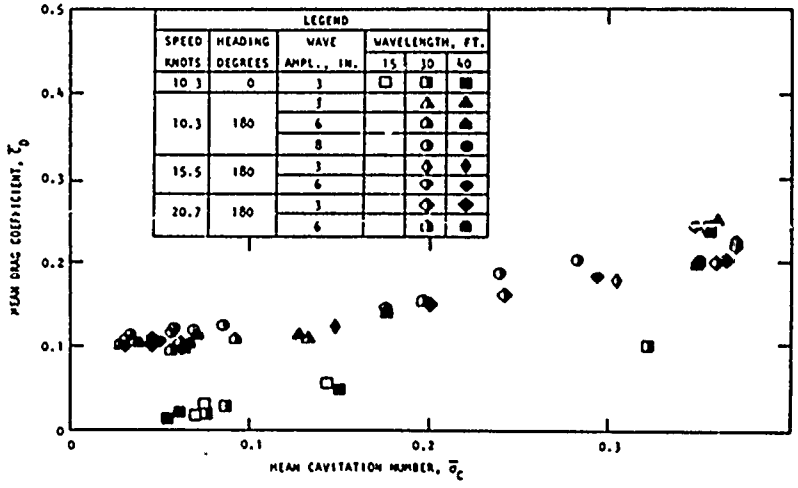

Figure 11h - 14.0 Degrees Angle of Attack, 2 Chords Depth.

Figure 11 - Continued

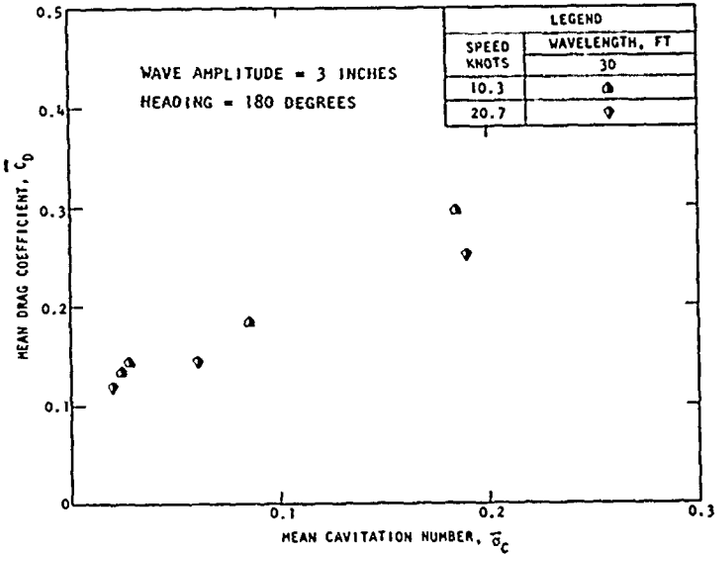

Figure 11i - 17.0 Degrees Angle of Attack, 1 Chord Depth.

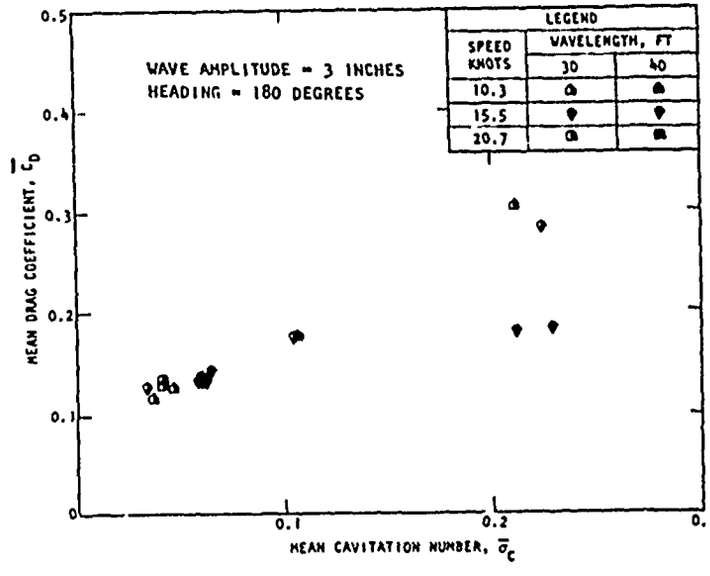

Figure 11j - 17.0 Degrees Angle of Attack, 2 Chords Depth.

Figure 12 - Variation of Oscillatory Lift Coefficient with Ventilation Index in Regular Waves.

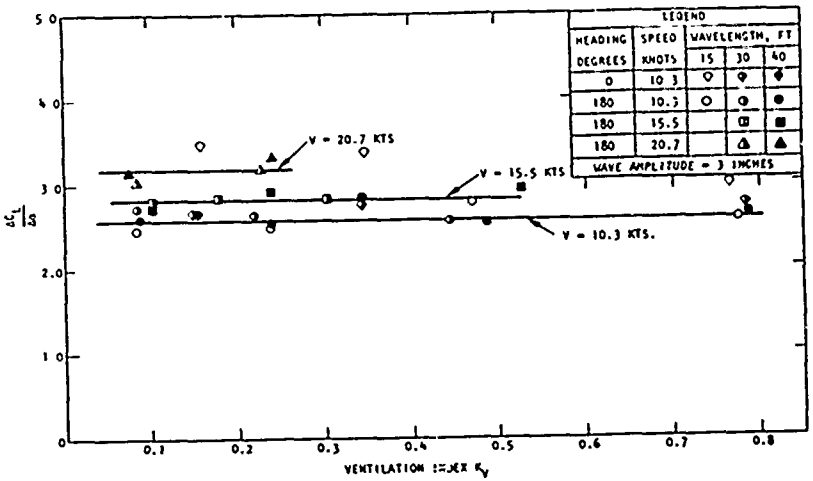

Figure 12a - 5.0 Degrees Angle of Attack, 1 Chord Depth.

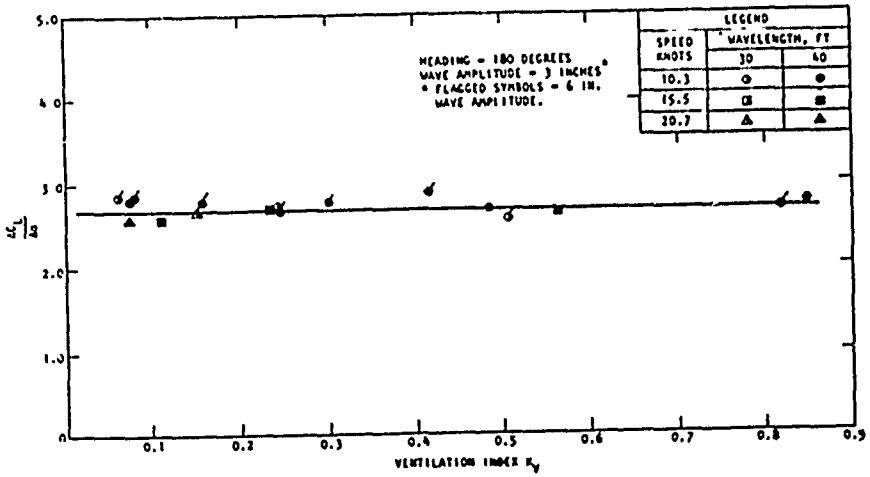

Figure 12c - 5.0 Degrees Angle of Attack, 3 Chords Depth.

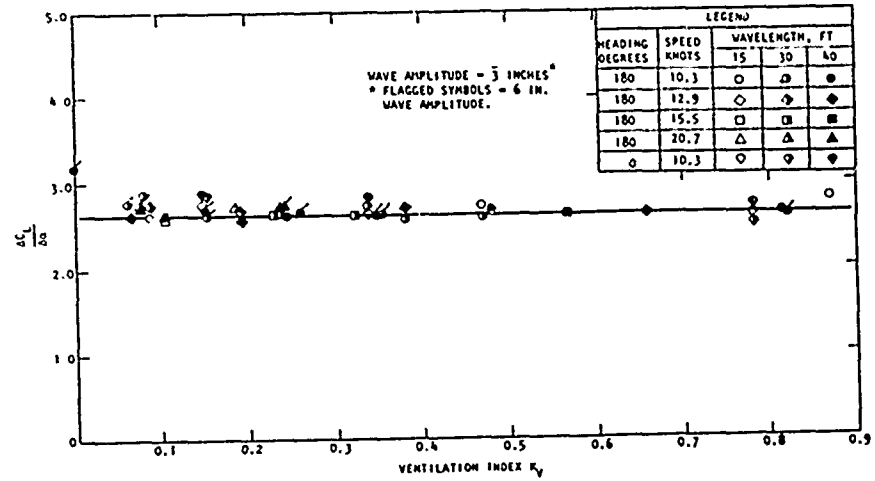

Figure 12b - 5.0 Degrees Angle of Attack, 2 Chords Depth.

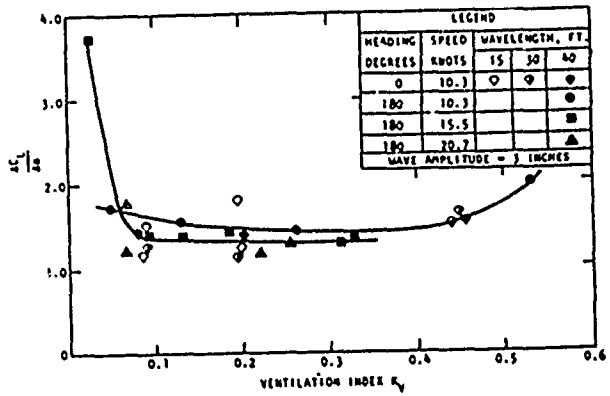

Figure 12d - 10.0 Degrees Angle of Attack, 1 Chord Depth.

Figure 12 - Continued

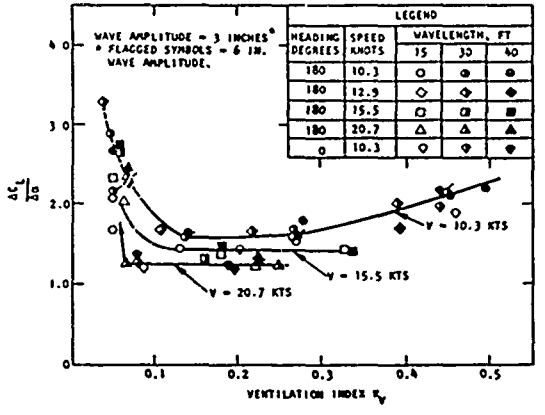

Figure 12e - 10.0 Degrees Angle of Attack, 2 Chords Depth.

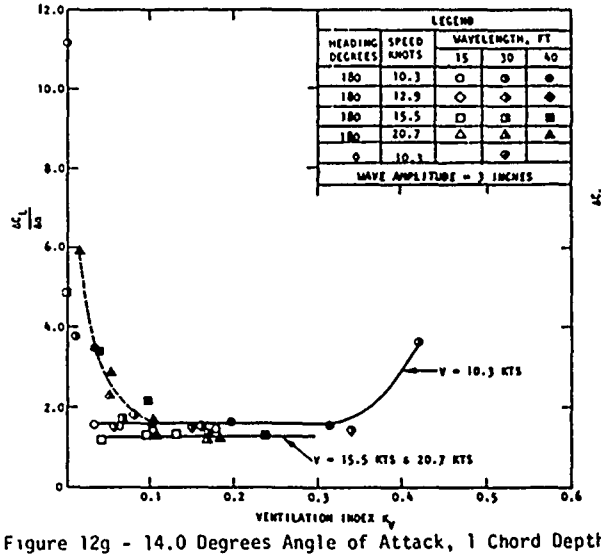

Figure 12g - 14.0 Degrees Angle of Attack, 1 Chord Depth.

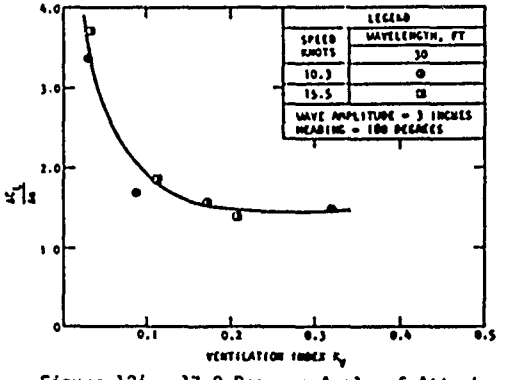

Figure 12i - 17.0 Degrees Angle of Attack, 1 Chord Depth.

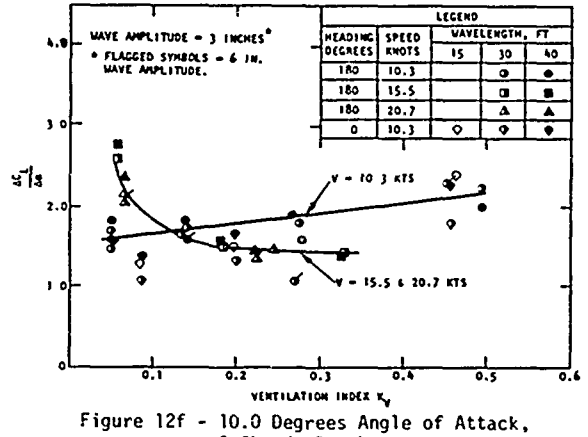

Figure 12f - 10.0 Degrees Angle of Attack, 3 Chords Depth.

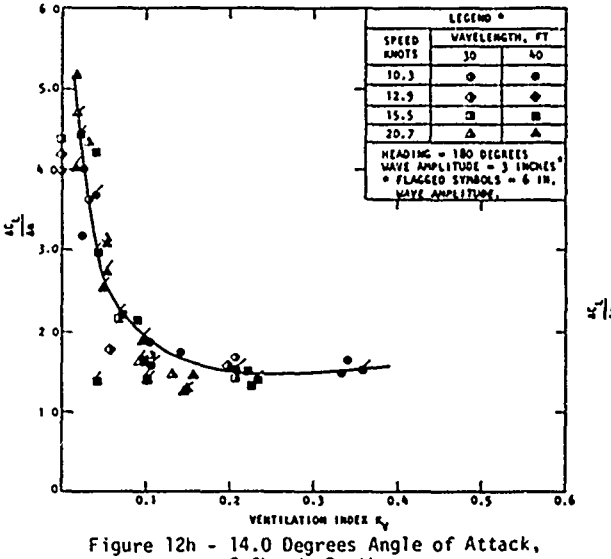

Figure 12h - 14.0 Degrees Angle of Attack, 2 Chords Depth.

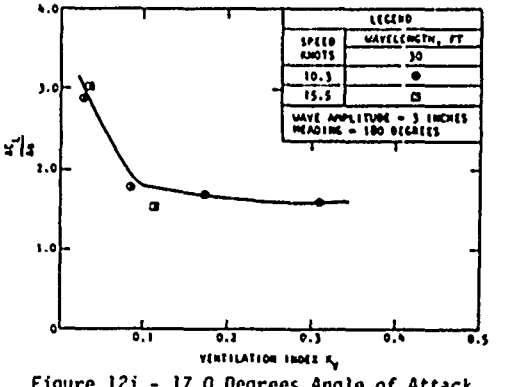

Figure 12j - 17.0 Degrees Angle of Attack, 2 Chords Depth.

Figure 13 - Variation of Oscillatory Drag Coefficient with Ventilation Index in Regular Waves.

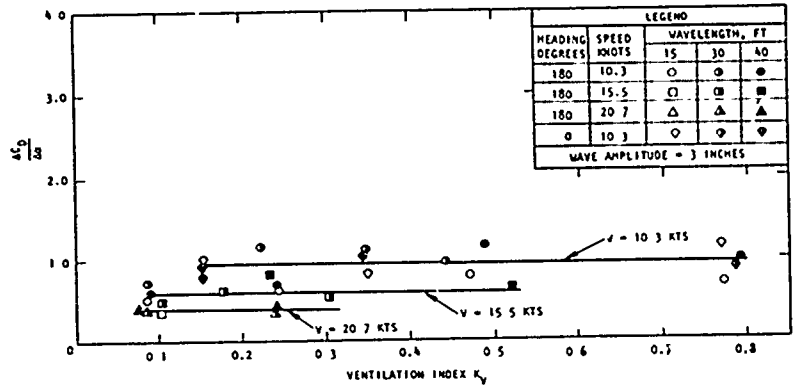

Figure 13a - 5.0 Degrees Angle of Attack, 1 Chord Depth.

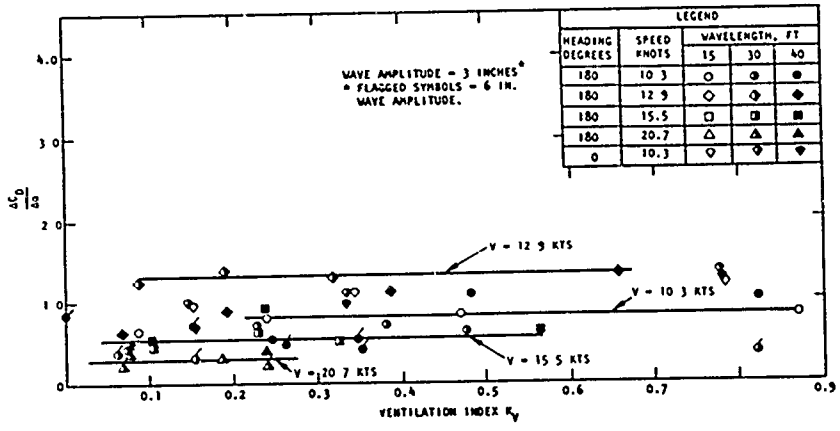

Figure 13b - 5.0 Degrees Angle of Attack, 2 Chords Depth.

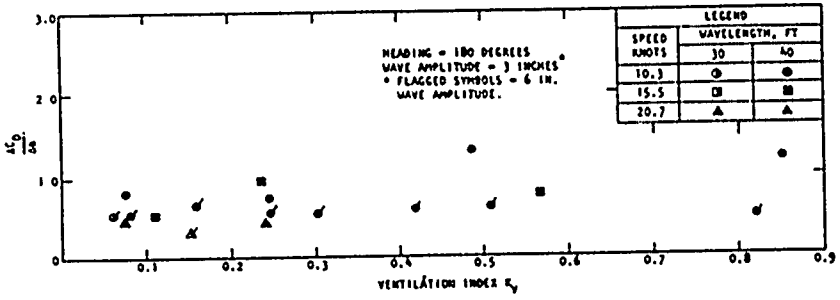

Figure 13c - 5.0 Degrees Angle of Attack, 3 Chords Depth.

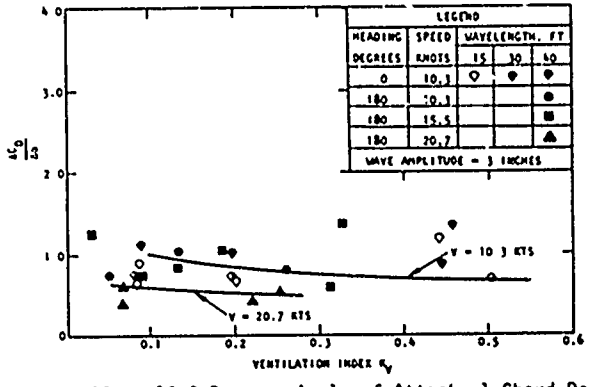

Figure 13d - 10.0 Degrees Angle of Attack, 1 Chord Depth.

Figure 13 Continued

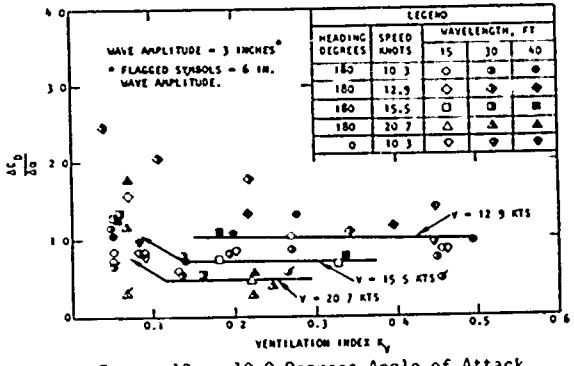

Figure 13e - 10.0 Degrees Angle of Attack, 2 Chords Depth.

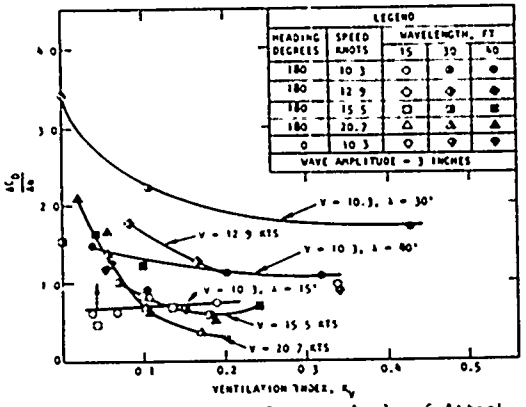

Figure 13g - 14.0 Degrees Angle of Attack, 1 Chord Depth.

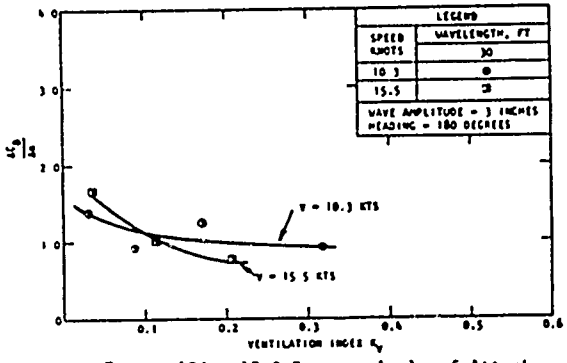

Figure 13i - 17.0 Degrees Angle of Attack, 1 Chord Depth.

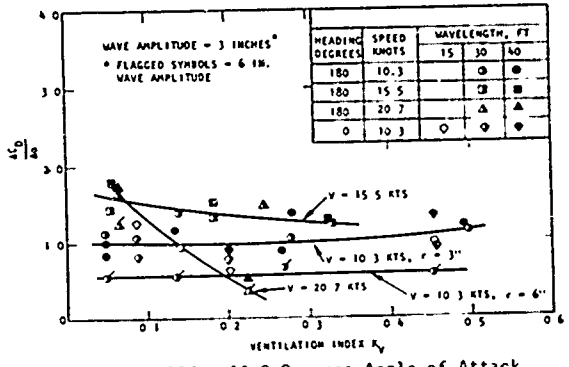

Figure 13f - 10.0 Degrees Angle of Attack, 3 Chords Depth.

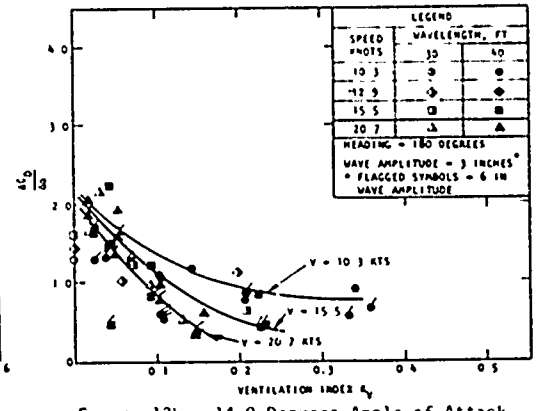

Figure 13h - 14.0 Degrees Angle of Attack, 2 Chords Depth.

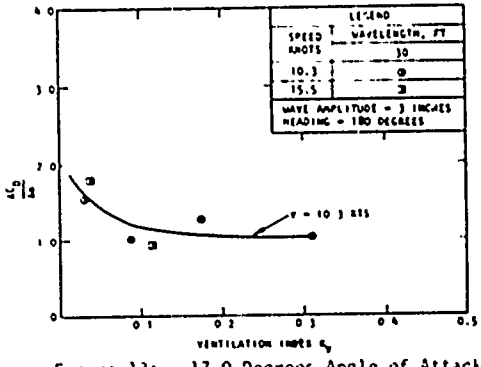

Figure 13j - 17.0 Degrees Angle of Attack, 2 Chords Depth.